Decoding rRNA sequences for improved metagenomics of sylvatic mosquito species

Cassandra Koh[1], Lionel Frangeul[1], Hervé Blanc[1], Carine Ngoagouni[2], Sébastien Boyer[3], Philippe Dussart[4], Nina Grau[5], Romain Girod[5], Jean-Bernard Duchemin[6] and Maria-Carla Saleh[1*]

[1] Viruses and RNA Interference Unit, Institut Pasteur, Université Paris Cité, CNRS UMR3569, Paris F-75015, France

[2] Medical Entomology Laboratory, Institut Pasteur de Bangui, Bangui PO Box 923, Central African Republic

[3] Medical and Veterinary Entomology Unit, Institut Pasteur du Cambodge, Phnom Penh 12201, Cambodia

[4] Virology Unit, Institut Pasteur du Cambodge, Phnom Penh 12201, Cambodia

[5] Medical Entomology Unit, Institut Pasteur de Madagascar, Antananarivo 101, Madagascar

[6] Vectopôle Amazonien Emile Abonnenc, Institut Pasteur de la Guyane, Cayenne 97306, French Guiana

* To whom correspondence should be addressed.

Present address: Philippe Dussart, Institut Pasteur de Madagascar, Antananarivo 101, Madagascar; Nina Grau, Sciences Economiques et Sociales de la Santé et Traitement de l'Information Médicale, Faculté de Médecine, Marseille 13005, France

Corresponding author: Maria-Carla Saleh, carla.saleh@pasteur.fr, +33 1 45 68 85 47.

ABSTRACT

As mosquito-borne virus epidemics are often preceded by undetected spillover events, surveillance and virus discovery studies in non-urban mosquitoes informs pre-emptive and responsive public health measures. RNA-seq metagenomics is a popular methodology but it is constrained by overabundant rRNA. The lack of reference sequences for most mosquito species is a major impediment against physical and computational removal of rRNA reads.

We describe a strategy to assemble novel rRNA sequences from mosquito specimens, producing an unprecedented dataset of 234 full-length 28S and 18S rRNA sequences of 33 medically important species from countries with known histories of mosquito-borne virus circulation (Cambodia, the Central African Republic, Madagascar, and French Guiana). We also evaluate the utility of rRNA sequences as molecular barcodes relative to the mitochondrial *cytochrome* c *oxidase I* (COI) gene. We show that rRNA sequences can be used for species identification when COI sequences are ambiguous or unavailable, revealing evolutionary relationships concordant with contemporary mosquito systematics.

This expansion of the rRNA reference library improves mosquito RNA-seq metagenomics by permitting the optimization of species-specific rRNA depletion protocols for a broader species range and streamlined species identification by rRNA barcoding. In addition, rRNA barcodes could serve as an additional tool for mosquito taxonomy and phylogeny.

Keywords: surveillance, RNA-seq, ribosomal RNA, barcode, metagenomics, mosquito

INTRODUCTION

Mosquitoes top the list of vectors for arthropod-borne diseases, being implicated in the transmission of many human pathogens responsible for arboviral diseases, malaria, and lymphatic filariasis (WHO, 2017). Mosquito-borne viruses circulate in sylvatic or urban transmission cycles driven by different mosquito species with their own distinct host preferences. Although urban mosquito species are chiefly responsible for amplifying epidemics in dense human populations, non-urban (sylvatic and peri-urban) mosquitoes maintain the transmission of these viruses among forest-dwelling animal reservoir hosts and are implicated in spillover events when humans enter their ecological niches (Valentine et al., 2019). Given that mosquito-borne virus emergence is preceded by such spillover events, continuous surveillance and virus discovery in non-urban mosquitoes is integral to designing effective public health measures to pre-empt or respond to mosquito-borne viral epidemics.

Metagenomics on field specimens is the most powerful method in the toolkit for understanding mosquito-borne disease ecology through the One Health lens (Webster et al., 2016). With next-generation sequencing becoming more accessible, such studies have provided unprecedented insights into the interfaces among mosquitoes, their environment, and their animal and human hosts. However, working with lesser studied mosquito species poses several problems.

First, metagenomics studies based on RNA-seq are bedevilled by overabundant ribosomal RNAs (rRNAs). These non-coding RNA molecules comprise at least 80% of the total cellular RNA population (Gale & Crampton, 1989). Due to their length and their abundance, they are a sink for precious next generation sequencing reads, decreasing the sensitivity of pathogen detection unless depleted during library preparation. Yet the most common rRNA depletion protocols require prior knowledge of rRNA sequences of the species of interest as they involve hybridizing antisense oligos to the rRNA molecules prior to removal by ribonucleases (Fauver et al., 2019; Phelps et al., 2021) or by bead capture (Kukutla et al., 2013). Presently, reference sequences for rRNAs are limited to only a handful of species from three genera: *Aedes*, *Culex*, and *Anopheles* (Ruzzante et al., 2019). The lack of reliable rRNA depletion methods could deter mosquito metagenomics studies from expanding their sampling diversity, resulting in a gap in our knowledge of mosquito vector ecology. The inclusion of lesser studied yet medically relevant non-urban species is therefore imperative.

Second, species identification based on morphology is notoriously complicated between members of species subgroups. This is especially the case among *Culex* subgroups. Sister species are often

sympatric and show at least some competence for a number of viruses, such as Japanese encephalitis virus, St Louis encephalitic virus, and Usutu virus (Nchoutpouen et al., 2019). Although they share many morphological traits, each of these species have distinct ecologies and host preferences, thus the challenge of correctly identifying vector species can affect epidemiological risk estimation for these diseases (Farajollahi et al., 2011). DNA molecular markers are often employed to a limited degree of success to distinguish between sister species (Batovska et al., 2017; Zittra et al., 2016).

To address the lack of full-length rRNA sequences in public databases, we sought to determine the 28S and 18S rRNA sequences of a diverse set of Old and New World non-urban (sylvatic and peri-urban) mosquito species from four countries representing three continents: Cambodia, the Central African Republic, Madagascar, and French Guiana. These countries, due to their proximity to the equator, contain high mosquito biodiversity (Foley et al., 2007) and have had long histories of mosquito-borne virus circulation. Increased and continued surveillance of local mosquito species could lead to valuable insights on mosquito virus biogeography. Using a unique score-based read filtration strategy to remove interfering non-mosquito rRNA reads for accurate *de novo* assembly, we produced a dataset of 234 novel full-length 28S and 18S rRNA sequences from 33 mosquito species, 30 of which have never been recorded before.

We also explored the functionality of 28S and 18S rRNA sequences as molecular barcodes by comparing their performance to that of the mitochondrial *cytochrome* c *oxidase subunit I* (COI) gene for molecular taxonomic and phylogenetic investigations. The COI gene is the most widely used DNA marker for molecular species identification and forms the basis of the Barcode of Life Data System (BOLD) (Hebert et al., 2003; Ratnasingham & Hebert, 2007). Presently, full-length rRNA sequences are much less represented compared to other molecular markers. We hope that our sequence dataset, with its species diversity and eco-geographical breadth, and the assembly strategy we describe would further facilitate the use of rRNA as barcodes. In addition, this dataset enables the design of species-specific oligos for cost-effective rRNA depletion for a broader range of mosquito species and streamlined molecular species diagnostics during RNA-seq.

RESULTS

Poor rRNA depletion using a non-specific depletion method

98 During library preparations of mosquito samples for RNA-seq, routinely used methods for depleting
99 rRNA are commercial kits optimised for human or mice samples (Belda et al., 2019; Bishop-Lilly et al.,
100 2010; Chandler et al., 2015; N. Kumar et al., 2012; Weedall et al., 2015; Zakrzewski et al., 2018) or
101 through 80–100 base pair antisense probe hybridisation followed by ribonuclease digestion (Fauver et
102 al., 2019; Phelps et al., 2021). In cases where the complete reference rRNA sequence of the target
103 species is not known, oligos would be designed based on the rRNA sequence of the closest related
104 species (25, this study). These methods should deplete the conserved regions of rRNA sequences.
105 However, the variable regions remain at abundances high enough to compromise RNA-seq output. In
106 our hands, we have found that using probes designed for the *Ae. aegypti* rRNA sequence followed by
107 RNase H digestion according to the protocol published by Morlan *et al.* (2012) produced poor
108 depletion in *Ae. albopictus*, and in Culicine and Anopheline species (Figure 1A). Additionally, the lack
109 of reference rRNA sequences compromises the *in silico* clean-up of remaining rRNA reads from
110 sequencing data, as reads belonging to variable regions would not be removed. To solve this and to
111 enable RNA-seq metagenomics on a broader range of mosquito species, we performed RNA-seq to
112 generate reference rRNA sequences for 33 mosquito species representing 10 genera from
113 Cambodia, the Central African Republic, Madagascar, and French Guiana. Most of these species are
114 associated with vector activity for various pathogens in their respective ecologies (Table 1).

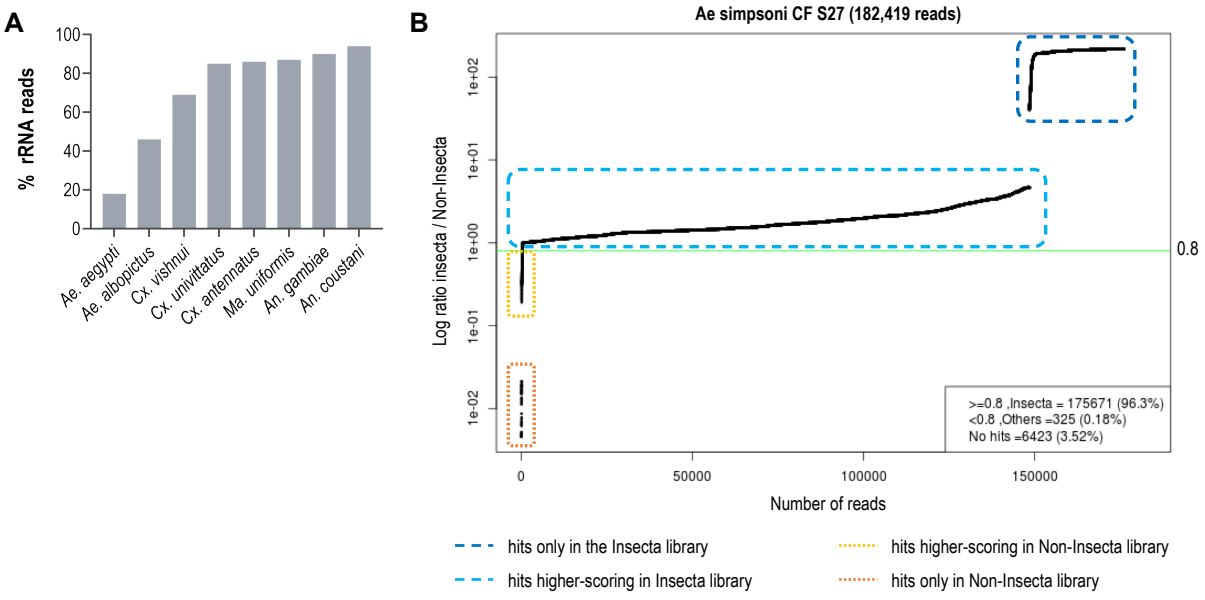

115

116 **Figure 1.** (**A**) Proportion of rRNA reads found in mosquito specimen pools of 5 individuals depleted by
117 probe hybridisation followed by RNase H digestion. Probes were antisense to *Ae. aegypti* rRNA

118 sequences. (**B**) Read vs. score ratio plot of a representative specimen “Ae simpsoni CS S27”. Green

119 line indicates 0.8 cut-off where only reads above this threshold are used in rRNA assembly.

120 **Table 1.** List of mosquito species represented in this study and their vector status.

Mosquito taxonomy*	Origin**	Collection site (ecosystem type)	Vector for***	Reference
Aedes (Fredardsius) vittatus	CF	rural (village)	DENV, ZIKV, CHIKV, YFV	(Diallo et al., 2020)
Aedes (Ochlerotatus) scapularis	GF	rural (village)	YFV	(Vasconcelos et al., 2001)
Aedes (Ochlerotatus) serratus	GF	rural (village)	YFV, OROV	(Cardoso et al., 2010; Gaillet et al., 2021)
Aedes (Stegomyia) aegypti	CF	urban	DENV, ZIKV, CHIKV, YFV	(Kraemer et al., 2019)
Aedes (Stegomyia) albopictus	CF, KH	rural (village, nature reserve)	DENV, ZIKV, CHIKV, YFV, JEV	(Auerswald et al., 2021; Kraemer et al., 2019)
Aedes (Stegomyia) simpsoni	CF	rural (village)	YFV	(Mukwaya et al., 2000)
Anopheles (Anopheles) baezai	KH	rural (nature reserve)	unreported	–
Anopheles (Anopheles) coustani	MG, CF	rural (village)	RVFV, malaria	(Mwangangi et al., 2013; Nepomichene et al., 2018; Ratovonjato et al., 2011)
Anopheles (Cellia) funestus	MG, CF	rural (village)	ONNV, malaria	(Lutomiah et al., 2013)
Anopheles (Cellia) gambiae	MG, CF	rural (village)	ONNV, malaria	(Brault et al., 2004)
Anopheles (Cellia) squamosus	MG	rural (village)	RVFV, malaria	(Ratovonjato et al., 2011; Stevenson et al., 2016)
Coquillettidia (Rhynchotaenia) venezuelensis	GF	rural (village)	OROV	(Gaillet et al., 2021)
Culex (Culex) antennatus	MG	rural (village)	RVFV	(Nepomichene et al., 2018; Ratovonjato et al., 2011)
Culex (Culex) duttoni	CF	rural (village)	unreported	–
Culex (Culex) neavei	MG	rural (village)	USUV	(Nikolay et al., 2011)
Culex (Culex) orientalis	KH	rural (nature reserve)	JEV	(Kim et al., 2015)
Culex (Culex) perexiguus	MG	rural (village)	WNV	(Vázquez González et al., 2011)
Culex (Culex) pseudovishnui	KH	rural (nature reserve)	JEV	(Auerswald et al., 2021; Maquart et al., 2021)
Culex (Culex) quinquefasciatus	MG, CF, KH	rural (village, nature reserve)	ZIKV, JEV, WNV, DENV, SLEV, RVFV, *Wuchereria bancrofti*	(Bhattacharya et al., 2016; Maquart et al., 2021; Ndiaye et al., 2016)
Culex (Culex) tritaeniorhynchus	MG, KH	rural (village, nature reserve)	JEV, WNV, RVFV	(Auerswald et al., 2021; Maquart et al., 2021)
Culex (Melanoconion) spissipes	GF	rural (village)	VEEV	(Weaver et al., 2004)
Culex (Melanoconion) portesi	GF	rural (village)	VEEV, TONV	(Talaga et al., 2021; Weaver et al., 2004)
Culex (Melanoconion) pedroi	GF	rural (village)	EEEV, VEEV, MADV	(Talaga et al., 2021; M. J. Turell et al., 2008)
Culex (Oculeomyia) bitaeniorhynchus	MG, KH	rural (village, nature reserve)	JEV	(Auerswald et al., 2021; Maquart et al., 2021)
Culex (Oculeomyia) poicilipes	MG	rural (village)	RVFV	(Ndiaye et al., 2016)
Eretmapodites intermedius	CF	rural (village)	unreported	–
Limatus durhamii	GF	rural (village)	ZIKV	(Barrio-Nuevo et al., 2020)

Mansonia (Mansonia) titillans	GF	rural (village)	VEEV, SLEV	(Hoyos-López et al., 2015; Michael J. Turell, 1999)
Mansonia (Mansonioides) indiana	KH	rural (nature reserve)	JEV	(Arunachalam et al., 2004)
Mansonia (Mansonioides) uniformis	MG, CF, KH	rural (village, nature reserve)	WNV, RVFV, *Wuchereria bancrofti*	(Lutomiah et al., 2013; Maquart et al., 2021; Ughasi et al., 2012)
Mimomyia (Etorleptiomyia) mediolineata	MG	rural (village)	unreported	–
Psorophora (Janthinosoma) ferox	GF	rural (village)	ROCV	(Mitchell et al., 1986)
Uranotaenia (Uranotaenia) geometrica	GF	rural (village)	unreported	–

* () indicates subgenus

** Origin countries are listed as their ISO alpha-2 codes: Central African Republic, CF; Cambodia, KH; Madagascar, MG; French Guiana, GF.

** dengue virus, DENV; Zika virus, ZIKV; chikungunya virus, CHIKV; Yellow Fever virus, YFV; Oropouche virus, OROV; Japanese encephalitis virus, JEV; Rift Valley Fever virus, RVFV; O'Nyong Nyong virus, ONNV; Usutu virus, USUV; West Nile virus, WNV; Saint Louis encephalitis virus, SLEV; Venezuelan equine encephalitis virus, VEEV; Tonate virus, TONV; Eastern equine encephalitis virus, EEEV; Madariaga virus, MADV; Rocio virus, ROCV.

rRNA reads filtering and sequence assembly

Assembling Illumina reads to reconstruct rRNA sequences from total mosquito RNA is not a straightforward task. Apart from host rRNA, total RNA samples also contain rRNA from other organisms associated with the host (microbiota, external parasites, or ingested diet). As rRNA sequences share high homology in conserved regions, Illumina reads (150 bp) from non-host rRNA can interfere with the contig assembly of host 28S and 18S rRNA.

Our score-based filtration strategy, described in detail in Methods, allowed us to bioinformatically remove interfering rRNA reads and achieve successful *de novo* assembly of 28S and 18S rRNA sequences for all our specimens. Briefly, for each Illumina read, we computed a ratio of BLAST scores against an Insecta library over a Non-Insecta library. Reads were segregated into four categories: (i) reads mapping only to the Insecta library, (ii) reads mapping better to the Insecta relative to Non-Insecta library, (iii) reads mapping better to the Non-Insecta relative to the Insecta library, and finally (iv) reads mapping only to the Non-Insecta library (Figure 1B, Supplementary Figure S1). By applying a conservative threshold of 0.8 to account for the non-exhaustiveness of the SILVA database, we removed reads that likely do not originate from mosquito rRNA. Notably, 15 of our specimens were engorged with vertebrate blood, a rich source of non-mosquito rRNA (Supplementary Table S1). The successful assembly of complete 28S and 18S rRNA sequences

demonstrates that this strategy performs as expected even with high amounts of non-host rRNA reads. This is particularly important in studies on field-captured mosquitoes as females are often sampled already having imbibed a blood meal or captured using the human landing catch technique.

We encountered challenges for three specimens morphologically identified as *Ma. africana* (Specimen ID 33-35). COI amplification by PCR did not produce any product, hence COI barcoding could not be used to confirm species identity. In addition, SPAdes was only able to assemble partial length contigs, despite the high number of reads with high scores against the Insecta library. Among other *Mansonia* specimens, the partial length contigs shared the highest similarity with contigs obtained from sample “Ma uniformis CF S51”. We then performed a guided assembly using the 28S and 18S sequences of this specimen as references, which successfully produced full-length contigs. In two of these specimens (Specimen ID 34 and 35), our assembly initially produced two sets of 28S and 18S rRNA sequences, one of which was similar to mosquito rRNA with low coverage and another with ten-fold higher coverage and 95% nucleotide sequence similarity to a water mite of genus *Horreolanus* known to parasitize mosquitoes. Our success in obtaining rRNA sequences for mosquito and water mite shows that our strategy can be applied to metabarcoding studies where the input material comprises multiple insect species, provided that appropriate reference sequences of the target species or of a close relative are available.

Altogether, we were able to assemble 122 28S and 114 18S full-length rRNA sequences for 33 mosquito species representing 10 genera sampled from four countries across three continents. This dataset contains, to our knowledge, the first records for 30 mosquito species and for seven genera: *Coquillettidia*, *Mansonia*, *Limatus*, *Mimomyia*, *Uranotaenia*, *Psorophora,* and *Eretmapodites*. Individual GenBank accession numbers for these sequences and specimen information are listed in Supplementary Table S1.

Comparative phylogeny of novel rRNA sequences relative to existing records

To verify the assembly accuracy of our rRNA sequences, we constructed a comprehensive phylogenetic tree from the 28S rRNA sequences generated from our study alongside those publicly available from GenBank (Figure 2). We applied a search criterion for GenBank sequences with at least 95% coverage of our sequence lengths (~4000 bp), aiming to represent as many species or genera as possible. Although we rarely found records for the same species included in our study, the resulting tree showed that our 28S sequences generally clustered according to their respective

176 species and subgenera, supported by moderate to good bootstrap support at terminal nodes. Species
177 taxa generally formed monophyletic clades, with the exception of *An. gambiae* and *Cx.*
178 *quinquefasciatus*. *An. gambiae* 28S rRNA sequences formed a clade with closely related sequences
179 from *An. arabiensis*, *An. merus*, and *An. coluzzii,* suggesting unusually high interspecies homology for
180 Anophelines or other members of subgenus *Cellia.* Meanwhile, *Cx. quinquefasciatus* 28S rRNA
181 sequences formed a taxon paraphyletic to sister species *Cx. pipiens*.

182

Figure 2. Phylogenetic tree based on 28S sequences generated from this study and from GenBank (3900 bp) as inferred using maximum-likelihood method and constructed to scale in MEGA X (S. Kumar et al., 2018). Values at each node indicate bootstrap support (%) from 500 replications. For sequences from this study, each specimen label contains information on taxonomy, origin (in 2-letter country codes), and specimen ID. Labels in bold indicate GenBank sequences with accession numbers shown. Label colours indicate genera: *Culex* in coral, *Anopheles* in purple, *Aedes* in dark blue, *Mansonia* in dark green, *Culiseta* in maroon, *Limatus* in light green, *Coquillettidia* in light blue, *Psorophora* in yellow, *Mimomyia* in teal, *Uranotaenia* in pink and *Eretmapodites* in brown. Scale bar at 0.05 is shown.

28S sequence-based phylogenetic reconstructions (Figure 2, with GenBank sequences; Supplementary Figure S3, this study only) showed marked incongruence to that of 18S sequences (Figure 3). Although all rRNA trees show the bifurcation of *Culicidae* into subfamilies *Anophelinae* and *Culicinae*, the recovered intergeneric phylogenetic relationships vary between the 28S and 18S trees and are weakly supported. The 18S tree also exhibited several taxonomic anomalies: (i) the lack of definitive clustering by species within the *Culex* subgenus (ii) the lack of distinction between 18S sequences of *Cx*. *pseudovishnui* and *Cx*. *tritaeniorhynchus*; (iii) the placement of Ma sp. 3 CF S35 within a *Culex* clade; and (iv) the lack of a monophyletic *Mimomyia* clade. The topology of the 18S tree suggests higher sequence divergence between the two *Cx. quinquefasciatus* taxa and between the two *Mimomyia* taxa than in the 28S trees. However, 28S and 18S rRNA sequences are encoded by linked loci in rDNA clusters and should not be analysed separately.

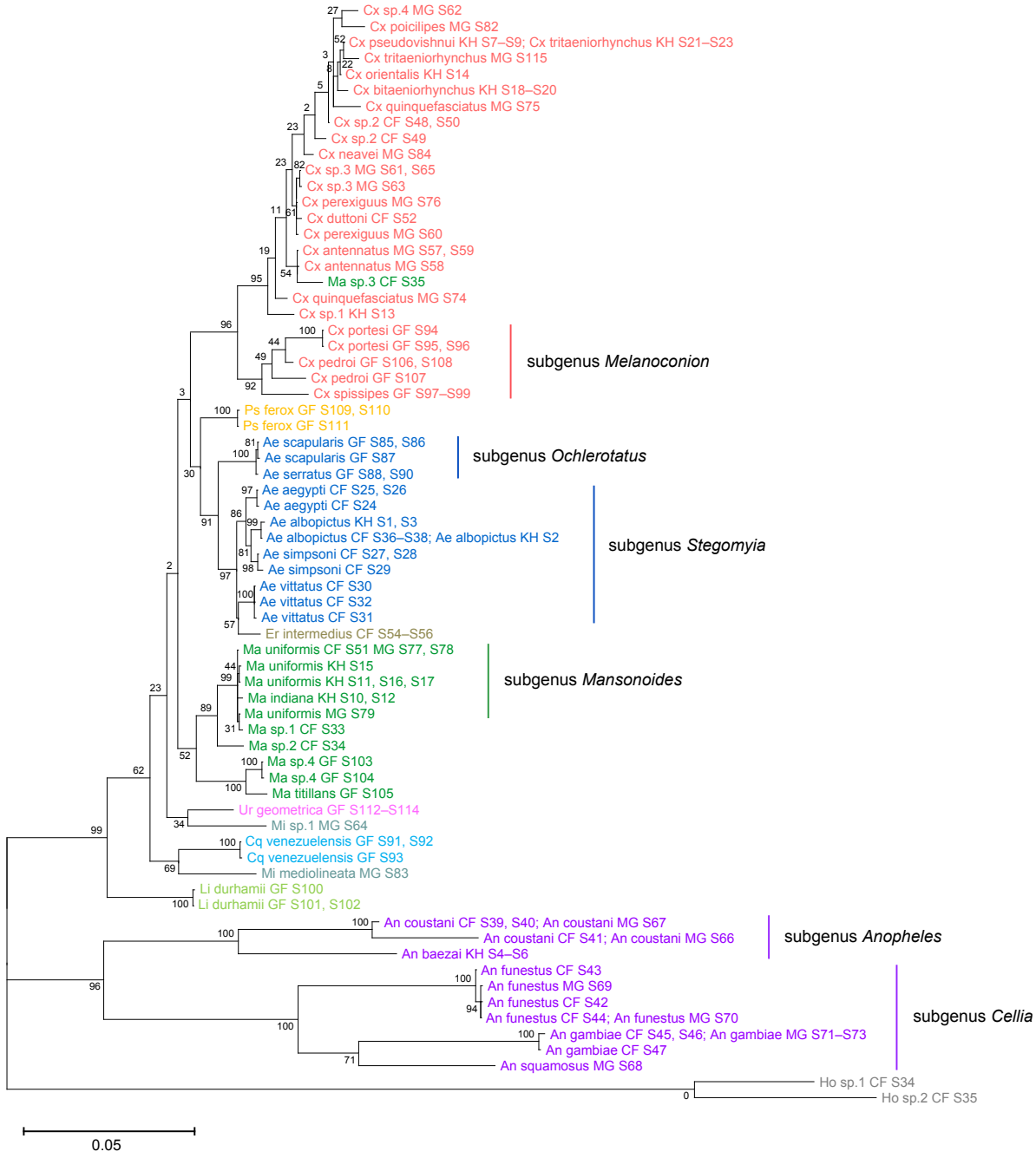

Figure 3. Phylogenetic tree based on 18S sequences (1900 bp) as inferred using maximum-likelihood method and constructed to scale in MEGA X (S. Kumar et al., 2018). Values at each node indicate bootstrap support (%) from 500 replications. Each specimen label contains information on taxonomy, origin (in 2-letter country codes), and specimen ID. Label colours indicate genera: *Culex* in coral, *Anopheles* in purple, *Aedes* in dark blue, *Mansonia* in dark green, *Limatus* in light green, *Coquillettidia* in light blue, *Psorophora* in yellow, *Mimomyia* in teal, *Uranotaenia* in pink and *Eretmapodites* in brown. Scale bar at 0.05 is shown.

Indeed, when concatenated 28S+18S rRNA sequences were generated from the same specimens (Figure 4), the phylogenetic tree resulting from these sequences more closely resembles the 28S tree (Figure 2) with regard to the basal position of the *Mimomyia* clade within the *Culicinae* subfamily with good bootstrap support in either tree (84% in 28S tree, 100% in concatenated 28S+18S tree). For internal nodes, bootstrap support values were higher in the concatenated tree compared to the 28S tree. Interestingly, the 28S+18S tree formed an *Aedini* tribe-clade encompassing taxa from genera *Psorophora, Aedes,* and *Eretmapodites*, possibly driven by the inclusion of 18S sequences. Concatenation also resolved the anomalies found in the 18S tree and added clarity to the close relationship between *Culex* and *Mansonia* taxa. Of note, relative to the 28S tree (Figure 2) the *Culex* and *Mansonia* genera are no longer monophyletic in the concatenated 28S+18S tree (Figure 4). Genus *Culex* is paraphyletic with respect to subgenus *Mansonoides* of genus *Mansonia* (Figure 2). *Ma*. *titillans* and Ma sp. 4, which we suspect to be *Ma. pseudotitillans,* always formed a distinct branch in 28S or 18S phylogenies, thus possibly representing a clade of subgenus *Mansonia*.

The concatenated 28S+18S tree recapitulates what is classically known about the systematics of our specimens, namely (i) the early divergence of subfamily *Anophelinae* from subfamily *Culicinae*, (ii) the division of genus *Anopheles* into two subgenera, *Anopheles* and *Cellia,* (iii) the division of genus *Aedes* into subgenera *Stegomyia* and *Ochlerotatus*, (iv) the divergence of monophyletic subgenus *Melanoconion* within the *Culex* genus (Harbach, 2007; Harbach & Kitching, 2016).

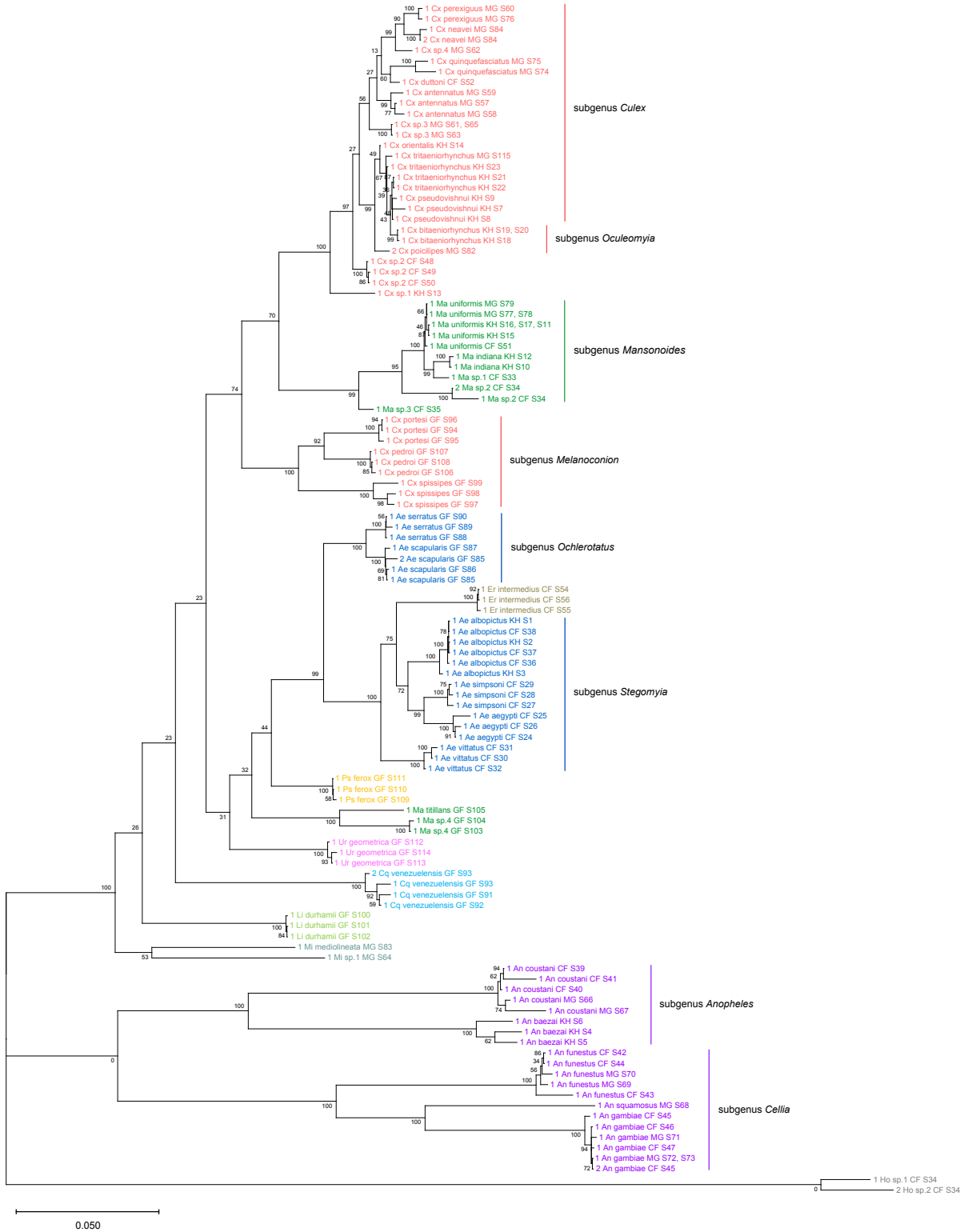

229

230 **Figure 4.** Phylogenetic tree based on concatenated 28S and 18S sequences generated from this
231 study (3900+1900 bp) as inferred using maximum-likelihood method and constructed to scale in
232 MEGA X (S. Kumar et al., 2018). Values at each node indicate bootstrap support (%) from 500
233 replications. For sequences from this study, each specimen label contains information on taxonomy,
234 origin (as indicated in 2-letter country codes), and specimen ID. Label colours indicate genera: *Culex*

in coral, *Anopheles* in purple, *Aedes* in dark blue, *Mansonia* in dark green, *Culiseta* in maroon, *Limatus* in light green, *Coquillettidia* in light blue, *Psorophora* in yellow, *Mimomyia* in teal, *Uranotaenia* in pink and *Eretmapodites* in brown. Scale bar at 0.05 is shown.

rRNA as a molecular marker for taxonomy and phylogeny

We sequenced a 621 bp region of the COI gene to confirm morphological species identification of our specimens and to compare the functionality of rRNA and COI sequences as molecular markers for taxonomic and phylogenetic investigations. COI sequences were able to unequivocally determine the species identity in most specimens except for the following cases. *An. coustani* COI sequences from our study regardless of specimen origin shared remarkably high nucleotide similarity (>98%) with several other *Anopheles* species such as *An. rhodesiensis*, *An. rufipes*, *An. ziemanni*, *An. tenebrosus*, although *An. coustani* remained the most frequent and closest match. In the case of *Ae. simpsoni*, three specimens had been morphologically identified as *Ae. opok* although their COI sequences showed 97–100% similarity to that of *Ae. simpsoni.* As GenBank held no records of *Ae. opok* COI at the time of this study, we instead aligned the putative *Ae. simpsoni* COI sequences against two sister species of *Ae. opok*: *Ae. luteocephalus* and *Ae. africanus.* We found they shared only 90% and 89% similarity, respectively. Given this significant divergence, we concluded these specimens to be *Ae. simpsoni*. Ambiguous results were especially frequent among *Culex* specimens belonging to the *Cx. pipiens* or *Cx. vishnui* subgroups, where the query sequence differed with either of the top two hits by a single nucleotide. For example, between *Cx. quinquefasciatus* and *Cx. pipiens* of the *Cx. pipiens* subgroup, and between *Cx. vishnui* and *Cx. tritaeniorhynchus* of the *Cx. vishnui* subgroup.

Among our three specimens of *Ma. titillans*, two appeared to belong to a single species that is different but closely related to *Ma. titillans*. We surmised that these specimens could instead be *Ma. pseudotitillans* based on morphological similarity but were not able to verify this by molecular means as no COI reference sequence is available for this species. These specimens are hence putatively labelled as “Ma sp.4”.

Phylogenetic reconstruction based on the COI sequences showed clustering of all species taxa into distinct clades, underlining the utility of the COI gene in molecular taxonomy (Figure 5)(Hebert et al., 2003; Ratnasingham & Hebert, 2007). However, species delineation among members of *Culex* subgroups were not as clear cut, although sister species were correctly placed as sister taxa. This is

264 comparable to the 28S+18S tree (Figure 4) and is indicative of lower intraspecies distances relative to
265 interspecies distances.

266 To evaluate the utility of 28S and 18S rRNA sequences for molecular taxonomy, we used the
267 28S+18S rRNA tree to discern the identity of six specimens for which COI barcoding could not be
268 performed. These specimens include three unknown *Mansonia* species (Specimen ID 33–35), a *Ma.*
269 *uniformis* (Specimen ID 51), an *An. gambiae* (Specimen ID 47), and a *Ur. geometrica* (Specimen ID
270 113). Their positions in the 28S+18S rRNA tree relative to adjacent taxa confirms the morphological
271 identification of all six specimens to the genus level and, for three of them, to the species level (Figure
272 4).

273 The phylogenetic relationships indicated by the COI tree compared to the 28S+18S tree present
274 only a few points of congruence. COI-based phylogenetic inference indeed showed clustering of
275 generic taxa into monophyletic clades albeit with very weak bootstrap support, except for genera
276 *Culex* and *Mansonia* (Figure 5). Contrary to the 28S+18S tree (Figure 4), *Culex* subgenus
277 *Melanoconion* was depicted as a polyphyletic taxon with *Cx. spissipes* being a part of the greater
278 *Culicini* clade with members from subgenera *Oculeomyia* and *Culex* while *Cx. pedroi* and *Cx. portesi*
279 formed a distantly related clade. Among the *Mansonia* specimens, the two unknown Ma sp.4
280 specimens were not positioned as the nearest neighbours of *Ma. titillans* and instead appeared to
281 have diverged earlier from most of the other taxa from the *Culicidae* family. Notably, the COI
282 sequences of genus *Anopheles* is not basal to the other members of *Culicidae* and is instead shown
283 to be sister to Culex COI sequences (8% bootstrap support). This is a direct contrast to what is
284 suggested by the rRNA phylogenies (Figures 2–4), which suggests *Culex* rRNA sequences to be
285 among the most recently diverged. Bootstrap support for the more internal nodes of the COI trees
286 were remarkably low compared to those of rRNA-based trees.

287 In all rRNA trees, it is clear that the interspecific and intersubgeneric evolutionary distances within
288 the genus *Anopheles* are high relative to any other genera, indicating a greater degree of divergence.
289 This is evidenced by the longer branch lengths connecting Anopheline species-clades to the node of
290 the most recent common ancestor for subgenera *Anopheles* and *Cellia* (Figures 2-4, Supplementary
291 Figure S3). This feature is not evident in the COI tree, where the Anopheline interspecies distances
292 are comparable to those within the *Culex*, *Aedes*, and *Mansonia* taxa.

Figure 5. Phylogenetic tree based on COI sequences (621–699 bp) as inferred using maximum-likelihood method and constructed to scale in MEGA X (S. Kumar et al., 2018). Values at each node indicate bootstrap support (%) from 500 replications. Each specimen label contains information on taxonomy, origin (as indicated in 2-letter country codes), and specimen ID. Label colours indicate genera: *Culex* in coral, *Anopheles* in purple, *Aedes* in dark blue, *Mansonia* in dark green, *Limatus* in

light green, *Coquillettidia* in light blue, *Psorophora* in yellow, *Mimomyia* in teal, *Uranotaenia* in pink and *Eretmapodites* in brown. Scale bar at 0.05 is shown.

On *Culex* subgroups

Culex (subgenus *Culex*) specimens of this study comprise several closely related sister species belonging to the *Cx. vishnui* and *Cx. univittatus* subgroups, which are notoriously difficult to differentiate based on morphology. Accordingly, in the 28S+18S rRNA (Figure 4) and COI (Figure 5) trees these species and their known sister species were clustered together within the *Culex* (subgenus *Culex*) clade: *Cx. tritaeniorhynchus* with *Cx. pseudovishnui* (*Cx. vishnui* subgroup); *Cx. perexiguus* with *Cx. neavei* (*Cx. univittatus* subgroup).

The use of COI barcoding to distinguish between members of the *Culex* subgroups was limited. For example, for the two *Cx. quinquefasciatus* samples in our taxonomic assemblage (Specimen ID 74 and 75), BLAST analyses of their COI sequences revealed they are a single nucleotide away from *Cx. pipiens* or *Cx. quinquefasciatus* COI sequences (Supplementary Table S2). In the 28S rRNA tree with GenBank sequences (Figure 2), two GenBank sequences of *Cx. pipiens* sequences formed a clade sister to another containing three *Cx. quinquefasciatus* GenBank sequences and the “Cx quinquefasciatus MG S74” sequence with 78% bootstrap support. This is in accordance with other studies examining mitochondrial sequences (Sun et al., 2019) and morphological attributes (Harbach et al., 2017). This shows that the 28S rRNA sequence can distinguish the two species and confirms that “Cx quinquefasciatus MG S74” is indeed a *Cx. quinquefasciatus* specimen. However, “Cx quinquefasciatus MG S75” is shown to be basal from other sequences within this *Cx. pipiens* subgroup-clade with 100% bootstrap support. Given that *Cx. quinquefasciatus* and *Cx. pipiens* are known to interbreed, it is plausible that this individual is a hybrid of the two species (Farajollahi et al., 2011).

DISCUSSION

RNA-seq metagenomics on field-captured non-urban mosquitoes is a valuable tool for pre-empting mosquito-borne virus emergences through surveillance and virus discovery. However, the lack of reference rRNA sequences hinders good oligo-based depletion and efficient clean-up of RNA-seq data. Additionally, *de novo* assembly of rRNA sequences is complicated due to regions that are highly conserved across all distantly related organisms that could be present in a single specimen, i.e.,

328 microbiota, parasites, or vertebrate blood meal. Hence, we sought to establish a method to
329 bioinformatically filter out non-host rRNA reads for the accurate assembly of novel 28S and 18S rRNA
330 reference sequences.
331 We found that phylogenetic reconstructions based on 28S sequences or concatenated 28S+18S
332 rRNA sequences were able to correctly cluster mosquito taxa according to species and corroborate
333 current mosquito classification. This demonstrates that our bioinformatics methodology reliably
334 generates bona fide 28S and 18S rRNA sequences, even in specimens parasitized by water mites or
335 engorged with vertebrate blood. Further, we were able to use 28S+18S rRNA taxonomy for molecular
336 species identification when COI sequences were unavailable or ambiguous, thus supporting the use
337 of rRNA sequences as a barcode. They have the advantage of circumventing the need to additionally
338 isolate and sequence DNA from specimens, as RNA-seq reads can be directly mapped against
339 reference sequences. Post-depletion, in our hands there are sufficient numbers of remaining reads
340 (5–10% of reads per sample) for assembly of complete rRNA contigs (unpublished data).
341 Phylogenetic inferences based on 28S or 18S rRNA sequences alone do not recover the same
342 interspecific relationships. Relative to 28S sequences, we observed more instances where multiple
343 specimens have near-identical 18S rRNA sequences. This can occur for specimens belonging to the
344 same species, but also for conspecifics sampled from different geographic locations, such as *An.*
345 *coustani*, *An. gambiae*, or *Ae. albopictus.* More rarely, specimens from the same species subgroup,
346 such as *Cx. pseudovishnui* and *Cx. tritaeniorhynchus*, also shared 18S rRNA sequences. This was
347 surprising given that the 18S rRNA sequences in our dataset is 1900 bp long. Concatenation of 28S
348 and 18S rRNA sequences resolved this issue, enabling species delineation even among sister
349 species of *Culex* subgroups, with which morphological identification meets its limits.
350 In Cambodia and other parts of Asia, the *Cx. vishnui* subgroup includes *Cx*. *tritaeniorhynchus*, *Cx*.
351 *vishnui*, and *Cx*. *pseudovishnui*, which are important vectors of JEV (Maquart & Boyer, 2022). The
352 former two were morphologically identified in our study but later revealed by COI barcoding to be a
353 sister species. Discerning sister species of the *Cx. pipiens* subgroup is further complicated by
354 interspecific breeding, with some populations showing genetic introgression to varying extents (Cornel
355 et al., 2003). The seven sister species of this subgroup are practically indistinguishable based on
356 morphology and require molecular methods to discern (Farajollahi et al., 2011; Zittra et al., 2016).
357 Indeed, the 621 bp COI sequence amplified in our study did not contain enough nucleotide

358 divergence to allow clear identification, given that the COI sequence of *Cx. quinquefasciatus*
359 specimens differed from that of *Cx. pipiens* by a single nucleotide. Batovska et al. (2017) found that
360 even the Internal Transcribed Spacer 2 (ITS2) rDNA region, another common molecular marker,
361 could not differentiate the two species. Other DNA molecular markers such as nuclear Ace-2 or CQ11
362 genes (Aspen & Savage, 2003; Zittra et al., 2016) or *Wolbachia pipientis* infection status (Cornel et
363 al., 2003) are typically employed in tandem. In our study, 28S rRNA sequence-based phylogeny
364 (Figure 2) validated the identity of specimen "Cx quinquefasciatus MG S74" and suggested that
365 specimen "Cx quinquefasciatus MG S75" might have been a *pipiens-quinquefasciatus* hybrid. These
366 examples demonstrate how 28S rRNA sequences, concatenated with 18S or alone, contain enough
367 resolution to differentiate between *Cx. pipiens* and *Cx. quinquefasciatus*. rRNA-based phylogeny thus
368 allows for more accurate species identification and ecological observations in the context of disease
369 transmission. Additionally, tracing the genetic flow across hybrid populations within the *Cx. pipiens*
370 subgroup can inform estimates of vectorial capacity for each species. As only one or two members
371 from the *Cx. pipiens* and *Cx. vishnui* subgroups were represented in our taxonomic assemblage, an
372 explicit investigation including all member species of these subgroups in greater sample numbers is
373 warranted to further test the degree of accuracy with which 28S and 18S rRNA sequences can
374 delineate sister species.

375 Our study included French Guianese *Culex* species *Cx. spissipes* (group Spissipes), *Cx. pedroi*
376 (group Pedroi), and *Cx. portesi* (group Vomerifer). These species belong to the New World subgenus
377 *Melanoconion*, section Spissipes, with well-documented distribution in North and South Americas
378 (Sirivanakarn, 1982) and are vectors of encephalitic alphaviruses EEEV and VEEV among others
379 (Talaga et al., 2021; M. J. Turell et al., 2008; Weaver et al., 2004). Indeed, our rooted rRNA and COI
380 trees showed the divergence of the three *Melanoconion* species from the major *Culex* clade
381 comprising species broadly found across Africa and Asia (Auerswald et al., 2021; Farajollahi et al.,
382 2011; Nchoutpouen et al., 2019; Takhampunya et al., 2011). The topology of the concatenated
383 28S+18S tree places the *Cx. portesi* and *Cx. pedroi* species-clades as sister groups (92% bootstrap
384 support), with *Cx. spissipes* as a basal group within the *Melanoconion* clade (100% bootstrap
385 support). This corroborates the systematics elucidated by Navarro and Weaver (2004) using the ITS2
386 marker, and those by Sirivanakarn (1982) and Sallum and Forattini (1996) based on morphology.
387 Curiously, in the COI tree, *Cx. spissipes* sequences were clustered with unknown species Cx. sp1,

388 forming a clade sister to another containing other *Culex* (*Culex*) and *Culex* (*Oculeomyia*) species,
389 albeit with very low bootstrap support. Previous phylogenetic studies based on the COI gene have
390 consistently placed *Cx. spissipes* or the Spissipes group basal to other groups within the
391 *Melanoconion* subgenus (Torres-Gutierrez et al., 2016, 2018). However, these studies contain only
392 *Culex* (*Melanoconion*) species in their assemblage, apart from *Cx. quinquefasciatus* to act as an
393 outgroup. This clustering of *Cx. spissipes* with non-*Melanoconion* species in our COI phylogeny could
394 be an artefact of a much more diversified assemblage rather than a true phylogenetic link.
395 Taking advantage of our multi-country sampling, we examined whether rRNA or COI phylogeny
396 can be used to discriminate conspecifics originating from different geographies. Our assemblage
397 contains five of such species: *An. coustani*, *An. funestus*, *An. gambiae*, *Ae. albopictus*, and *Ma.*
398 *uniformis*. Among the rRNA trees, the concatenated 28S+18S tree and 28S tree were able to
399 discriminate between *Ma. uniformis* specimens from Madagascar, Cambodia, and the Central African
400 Republic, and between *An. coustani* specimens from Madagascar and the Central African Republic
401 (100% bootstrap support). In the COI tree, only *Ma. uniformis* was resolved into geographical clades
402 comprising specimens from Madagascar and specimens from Cambodia (72% bootstrap support). No
403 COI sequence was obtained from one *Ma. uniformis* from the Central African Republic. The 28S+18S
404 rRNA sequences ostensibly provided more population-level genetic information than COI sequences
405 alone with better support. The use of rRNA sequences in investigating the biodiversity of mosquitoes
406 should therefore be explored with a more comprehensive taxonomic assemblage.
407 The phylogenetic reconstructions based on rRNA or COI sequences in our study are hardly
408 congruent, but two principal differences stand out. First, the COI phylogeny does not recapitulate the
409 early divergence of *Anophelinae* from *Culicinae* (Figure 5). This is at odds with other studies
410 estimating mosquito divergence times based on mitochondrial genes (Logue et al., 2013; Lorenz et
411 al., 2021) or nuclear genes (Reidenbach et al., 2009). The second notable feature in the rRNA trees is
412 the remarkably large interspecies and intersubgeneric evolutionary distances within genus *Anopheles*
413 relative to *Culicinae* genera (Figures 2–4, Supplementary Figure S4) but this is not apparent in the
414 COI tree. The hyperdiversity among *Anopheles* taxa may be attributed to the earlier diversification of
415 the *Anophelinae* subfamily in the early Cretaceous period compared to that of the *Culicinae* subfamily,
416 a difference of at least 40 million years (Lorenz et al., 2021). The differences in rRNA and COI tree
417 topologies indicate a limitation in using COI alone to determine evolutionary relationships. Importantly,

418 drawing phylogenetic conclusions from short DNA barcodes such as COI has been cautioned against
419 due to its weak phylogenetic signal (Hajibabaei et al., 2006). The relatively short length of our COI
420 sequences (621–699 bp) combined with the 100-fold higher nuclear substitution rate of mitochondrial
421 genomes relative to nuclear genomes (Arctander, 1995) could result in homoplasy (Danforth et al.,
422 2005), making it difficult to clearly discern ancestral sequences and correctly assign branches into
423 lineages, as evidenced by the poor nodal bootstrap support at genus-level branches. Indeed, in the
424 study by Lorenz et al. (2021), a phylogenetic tree constructed using a concatenation of all 13 protein-
425 coding genes of the mitochondrial genome was able to resolve ancient divergence events. This
426 affirms that while COI sequences can be used to reveal recent speciation events, longer or multi-gene
427 molecular markers are necessary for studies into deeper evolutionary relationships (Danforth et al.,
428 2005).

429 In contrast to Anophelines where 28S rRNA phylogenies illustrated higher interspecies divergence
430 compared to COI phylogeny, two specimens of an unknown *Mansonia* species, “Ma sp.4 GF S103”
431 and “Ma sp.4 GF S104”, provided an example where interspecies relatedness based on their COI
432 sequences is greater than that based on their rRNA sequences in relation to “Ma titillans GF S105”.
433 While all rRNA trees (Figure 2–4) placed “Ma titillans GF S105” as a sister taxon with 100% bootstrap
434 support, the COI tree placed Ma sp.4 basal to all other species except *Ur. geometrica*. This may hint
435 at a historical selective sweep in the mitochondrial genome, whether arising from geographical
436 separation, mutations, or linkage disequilibrium with inherited symbionts (Hurst & Jiggins, 2005),
437 resulting in the disparate mitochondrial haplogroups found in French Guyanese Ma sp.4 and *Ma.*
438 *titillans*. In addition, both haplogroups are distant from those associated with members of subgenus
439 *Mansonoides*. To note, the COI sequences of “Ma sp.4 GF S103” and “Ma sp.4 GF S104” share
440 87.12 and 87.39% nucleotide similarity, respectively, to that of “Ma titillans GF S105”. Interestingly,
441 the endosymbiont *Wolbachia pipientis* has been detected in *Ma. titillans* sampled from Brazil (De
442 Oliveira et al., 2015), which may contribute to the divergence of “Ma titillans GF S105” COI sequence
443 away from those of Ma sp.4. This highlights other caveats of using a mitochondrial DNA marker in
444 determining evolutionary relationships (Hurst & Jiggins, 2005), which nuclear markers such as 28S
445 and 18S rRNA sequences may be immune to.

446 **Conclusions**

RNA-seq metagenomics is a valuable tool for surveillance and virus discovery in non-urban mosquitoes but it is impeded by the lack of full-length rRNA reference sequences. Here we presented a rRNA sequence assembly strategy and 234 newly generated 28S and 18S mosquito rRNA sequences. Our work has expanded the current rRNA reference library by providing, to our knowledge, the first full-length rRNA records for 30 species in public databases and paves the way for the assembly of many more. These novel rRNA sequences can improve mosquito RNA-seq metagenomics by expanding reference sequence data for the optimization of species-specific oligo-based rRNA depletion protocols, for streamlined species identification by rRNA barcoding and for improved RNA-seq data clean-up. In addition, RNA barcodes could serve as an additional tool for mosquito taxonomy and phylogeny although further studies are necessary to reveal how they compare against other nuclear or mitochondrial DNA marker systems (Batovska et al., 2017; Beebe, 2018; Behura, 2006; Ratnasingham & Hebert, 2007; Reidenbach et al., 2009; Vezenegho et al., 2022).

We showed that phylogenetic inferences from a tree based on 28S rRNA sequences alone or concatenated 28S +18S rRNA sequences largely agree with contemporary mosquito classification and can be used for species diagnostics given a reference sequence. In analysing the same set of specimens by COI or rRNA sequences, we found deep discrepancies in phylogenetic inferences. We conclude that while COI-based phylogeny can reveal recent speciation events, rRNA sequences may be better suited for investigations of deeper evolutionary relationships as they are less prone to selective sweeps and homoplasy.

MATERIALS AND METHODS

Sample collection

Mosquito specimens were sampled from 2019 to 2020 by medical entomology teams from the Institut Pasteur de Bangui (Central African Republic, Africa; CF), Institut Pasteur de Madagascar (Madagascar, Africa; MG), Institut Pasteur du Cambodge (Cambodia, Asia; KH), and Institut Pasteur de la Guyane (French Guiana, South America; GF). Adult mosquitoes were sampled using several techniques including CDC light traps, BG sentinels, and human-landing catches. Sampling sites are non-urban locations including rural settlements in the Central African Republic, Madagascar, and French Guiana and national parks in Cambodia. Mosquitoes were identified using morphological

identification keys on cold tables before preservation by flash freezing in liquid nitrogen and transportation in dry ice to Institut Pasteur Paris for analysis. A list of the 112 mosquito specimens included in our taxonomic assemblage and their related information are provided in Supplementary Table S1.

RNA and DNA isolation

Nucleic acids were isolated from mosquito specimens using TRIzol reagent according to manufacturer's protocol (Invitrogen, Thermo Fisher Scientific, Waltham, Massachusetts, USA). Single mosquitoes were homogenised into 200 µL of TRIzol reagent and other of the reagents within the protocol were volume-adjusted accordingly. Following phase separation, RNA were isolated from the aqueous phase while DNA were isolated from the remaining interphase and phenol-chloroform phase. From here, RNA is used to prepare cDNA libraries for next generation sequencing while DNA is used in PCR amplification and Sanger sequencing of the mitochondrial *cytochrome* c *oxidase subunit I* (COI) gene as further described below.

Probe depletion of rRNA

We tested a selective rRNA depletion protocol by Morlan *et al.* (2012) on several mosquito species from the *Aedes*, *Culex*, and *Anopheles* genera. We designed 77 tiled 80 bp DNA probes antisense to the *Ae. aegypti* 28S, 18S, and 5.8S rRNA sequences. A pool of probes at a concentration of 0.04 µM were prepared. To bind probes to rRNA, 1 µL of probes and 2 µL of Hybridisation Buffer (100 mM Tris-HCl and 200 mM NaCl) was added to rRNA samples to a final volume of 20 µL and subjected to a slow-cool incubation starting at 95 ºC for 2 minutes, then cooling to 22 ºC at a rate of 0.1 ºC per second, ending with an additional 5 minutes at 22 ºC. The resulting RNA:DNA hybrids were treated with 2.5 µL Hybridase™ Thermostable RNase H (Epicentre, Illumina, Madison, Wisconsin, USA) and incubated at 37 ºC for 30 minutes. To remove DNA probes, the mix was treated with 1 µL DNase I (Invitrogen) and purified with Agencourt RNAClean XP Beads (Beckman Coulter, Brea, California, USA). The resulting RNA is used for total RNA sequencing to check depletion efficiency.

Total RNA sequencing

To obtain rRNA sequences, RNA samples were quantified on a Qubit Fluorometer (Invitrogen) using the Qubit RNA BR Assay kit (Invitrogen) for concentration adjustment. Non-depleted total RNA was used for library preparation for next generation sequencing using the NEBNext Ultra II RNA Library

Preparation Kit for Illumina (New England Biolabs, Ipswich, Massachusetts, USA) and the NEBNext Multiplex Oligos for Illumina (Dual Index Primers Set 1) (New England Biolabs). Sequencing was performed on a NextSeq500 sequencing system (Illumina, San Diego, California, USA). Quality control of fastq data and trimming of adapters were performed with FastQC and cutadapt, respectively.

28S and 18S rRNA assembly

To obtain 28S and 18S rRNA contigs, we had to first clean our fastq library by separating the reads representing mosquito rRNA from all other reads. To achieve this, we used the SILVA RNA sequence database to create 2 libraries: one containing all rRNA sequences recorded under the "Insecta" node of the taxonomic tree, the other containing the rRNA sequences of many others nodes distributed throughout the taxonomic tree, hence named “Non-Insecta” (Quast et al., 2013). Each read was aligned using the nucleotide Basic Local Alignment Search Tool (BLASTn, **https://blast.ncbi.nlm.nih.gov/**) of the National Center for Biotechnology Information (NCBI) against each of the two libraries and the scores of the best high-scoring segment pairs from the two BLASTns are subsequently used to calculate a ratio of Insecta over Non-Insecta scores (Altschul et al., 1990). Only reads with a ratio greater than 0.8 were used in the assembly. The two libraries being non-exhaustive, we chose this threshold of 0.8 to eliminate only reads that were clearly of a non-insect origin. Selected reads were assembled with the SPAdes assembler using the “-rna” option, allowing more heterogeneous coverage of contigs and kmer lengths of 31 , 51 and 71 bases (Bankevich et al., 2012). This method successfully assembled rRNA sequences for all specimens, including a parasitic *Horreolanus* water mite (122 sequences for 28S and 114 sequences for 18S).

Initially, our filtration technique had two weaknesses. First, there is a relatively small number of complete rRNA sequences in the Insecta library from SILVA. To compensate for this, we carried out several filtration cycles, each time adding in the complete sequences produced in previous cycles to the Insecta library. Second, when our mosquito specimens were parasitized by other insects, it was not possible to bioinformatically filter out rRNA reads belonging to the parasite. For these rare cases, we used the " --trusted-contigs" option of SPAdes, giving it access to the 28S and 18S sequences of the mosquito closest in terms of taxonomic distance. By doing this, the assembler was able to reconstruct the rRNA of the mosquito as well as the rRNA of the parasitizing insect. All assembled rRNA sequences from this study have been deposited in GenBank with accession numbers

OM350214–OM350327 for 18S rRNA sequences and OM542339–OM542460 for 28S rRNA sequences.

COI amplicon sequencing

The mitochondrial COI gene was amplified from DNA samples using the universal "Folmer" primer set LCO1490 (5'- GGTCAACAAATCATAAAGATATTGG -3') and HCO2198 (5'-TAAACTTCAGGGTGACCAAAAAATCA-3'), as per standard COI barcoding practices, producing a 658 bp product (Folmer et al., 1994). PCRs were performed using Phusion High-Fidelity DNA Polymerase (Thermo Fisher Scientific). Every 50 µL reaction contained 10 µL of 5X High Fidelity buffer, 1 µL of 10 mM dNTPs, 2.5 µL each of 10 mM forward (LCO1490) and reverse (HCO2198) primer, 28.5 µL of water, 5 µL of DNA sample, and 0.5 µL of 2 U/µL Phusion DNA polymerase. A 3-step cycling incubation protocol was used: 98 ºC for 30 seconds; 35 cycles of 98 ºC for 10 seconds, 60 ºC for 30 seconds, and 72 ºC for 15 seconds; 72 ºC for 5 minutes ending with a 4 ºC hold. PCR products were size-verified using gel electrophoresis and then gel-purified using the QIAquick Gel Extraction Kit (Qiagen, Hilden, Germany). Sanger sequencing of the COI amplicons were performed by Eurofins Genomics, Ebersberg, Germany.

COI sequence analysis

Forward and reverse COI DNA sequences were end-trimmed to remove bases of poor quality (Q score < 30). At the 5' ends, sequences were trimmed at the same positions such that all forward sequences start with 5'- TTTTGG and all reverse sequences start with 5'- GGNTCT. Forward and reverse sequences were aligned using BLAST to produce a 621 bp consensus sequence. In cases where good quality sequences extends beyond 621 bp, forward and reverse sequences were assembled using Pearl (**https://www.gear-genomics.com/pearl/**) and manually checked for errors against trace files (Rausch et al., 2019, 2020). We successfully assembled a total of 106 COI sequences. All assembled COI sequences from this study have been deposited in GenBank with accession numbers OM630610–OM630715.

COI validation of morphology-based species identification

We analysed assembled COI sequences with BLASTn against the nucleotide collection (nr/nt) database to confirm morphology-based species identification. BLAST analyses revealed 32 cases where top hits indicated a different species identity, taking <95% nucleotide sequence similarity as the

564 threshold to delineate distinct species (Supplementary Table S2). In these cases, the COI sequence
565 of the specimen was then BLAST-aligned against a GenBank record representing the morphological
566 species to verify that the revised identity is a closer match by a significant margin, i.e., more than 2%
567 nucleotide sequence similarity. All species names reported hereafter reflect identities determined by
568 COI barcoding except for cases where COI-based identities were ambiguous, in which case
569 morphology-based identities were retained. In cases where matches were found within a single genus
570 but of multiple species, specimens were indicated as an unknown member of their genus (e.g., *Culex*
571 sp.). Information of the highest-scoring references for all specimens, including details of ambiguous
572 BLASTn results, are recorded in Supplementary Table S2.
573 Within our COI sequences, we found six unidentified *Culex* species (including two that matched to
574 GenBank entries identified only to the genus level), four unidentified *Mansonia* species, and one
575 unidentified *Mimomyia* species. For *An. baezai*, no existing GenBank records were found at the time
576 this analysis was performed.

577 **Phylogenetic analysis**

578 Multiple sequence alignment (MSA) were performed on assembled COI and rRNA sequences using
579 the MUSCLE software (Supplementary Files 1–4) (Edgar, 2004; Madeira et al., 2019). As shown in
580 Supplementary Figure S2, the 28S rRNA sequences contain many blocks of highly conserved
581 nucleotides, which makes the result of multiple alignment particularly obvious. We therefore did not
582 test other alignment programs. The multiple alignment of the COI amplicons is even more evident
583 since no gaps are necessary for this alignment.
584 Phylogenetic tree reconstructions were performed with the MEGA X software using the maximum-
585 likelihood method (S. Kumar et al., 2018). Default parameters were used with bootstrapping with 500
586 replications to quantify confidence level in branches. For rRNA trees, sequences belonging to an
587 unknown species of parasitic water mite (genus *Horreolanus*) found in our specimens served as an
588 outgroup taxon. In addition, we created and analysed a separate dataset combining our 28S rRNA
589 sequences and full-length 28S rRNA sequences from GenBank totalling 169 sequences from 58
590 species (12 subgenera). To serve as outgroups for the COI tree, we included sequences obtained
591 from GenBank of three water mite species, *Horreolanus orphanus* (KM101004), *Sperchon fuxiensis*
592 (MH916807), and *Arrenurus* sp. (MN362807).

DECLARATIONS

Availability of data and materials

Raw RNA-seq fastq sequence data are available from the corresponding author upon reasonable request. Multiple sequence alignment files are included as supplementary files. All sequences generated in this study have been deposited in GenBank under the accession numbers OM350214–OM350327 for 18S rRNA sequences, OM542339–OM542460 for 28S rRNA sequences, and OM630610–OM630715 for COI sequences (Supplementary Table S1).

Competing interests

The authors declare that they have no financial or non-financial competing interests.

Funding

This work was supported by the Defence Advanced Research Projects Agency PREEMPT program managed by Dr. Rohit Chitale and Dr. Kerri Dugan [Cooperative Agreement HR001118S0017] (the content of the information does not necessarily reflect the position or the policy of the U.S. government, and no official endorsement should be inferred).

Acknowledgements

We thank members of the Saleh lab for valuable discussions and to Dr Louis Lambrechts for critical reading of the manuscript. We especially thank all medical entomology staff of IP Bangui, IP Cambodge (Sony Yean, Kimly Heng, Kalyan Chhuoy, Sreynik Nhek, Moeun Chhum, Kimhuor Sour and Pierre-Olivier Maquart), IP Madagascar, and IP Guyane for assistance in field missions, laboratory work, and logistics, and Inès Partouche from IP Paris for laboratory assistance. We are also grateful to Dr Catherine Dauga for advice on phylogenetic analyses, and to Amandine Guidez for providing a French Guiana-specific COI reference library.

SUPPLEMENTARY FILES

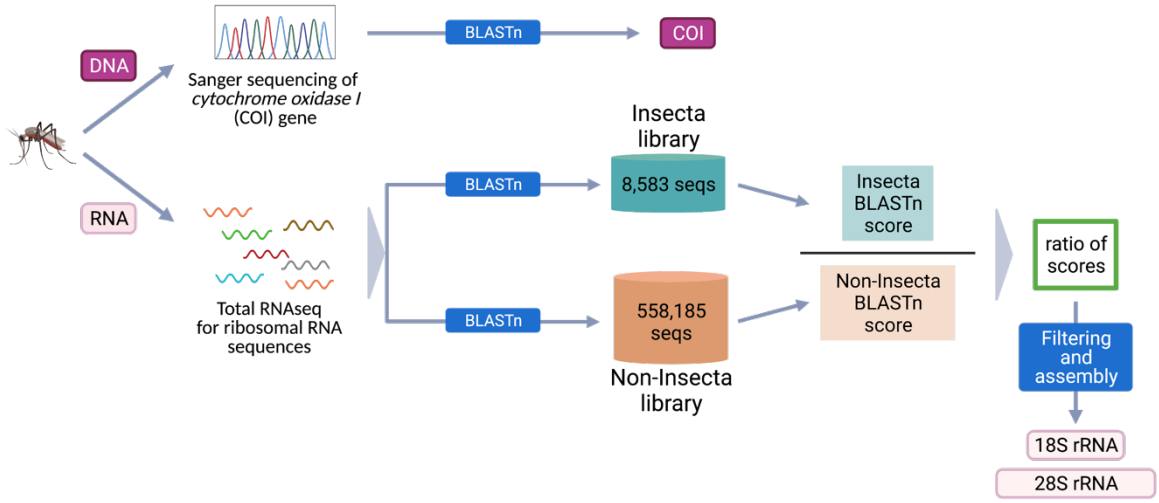

Supplementary Figure S1. Study workflow from specimens to sequences.

Supplementary Table S1. Taxonomic and sampling information on mosquito specimens and associated accession numbers of their 28S, 18S, and COI sequences (XLSX).

Supplementary Table S2. COI sequence BLAST analyses summary (XLSX).

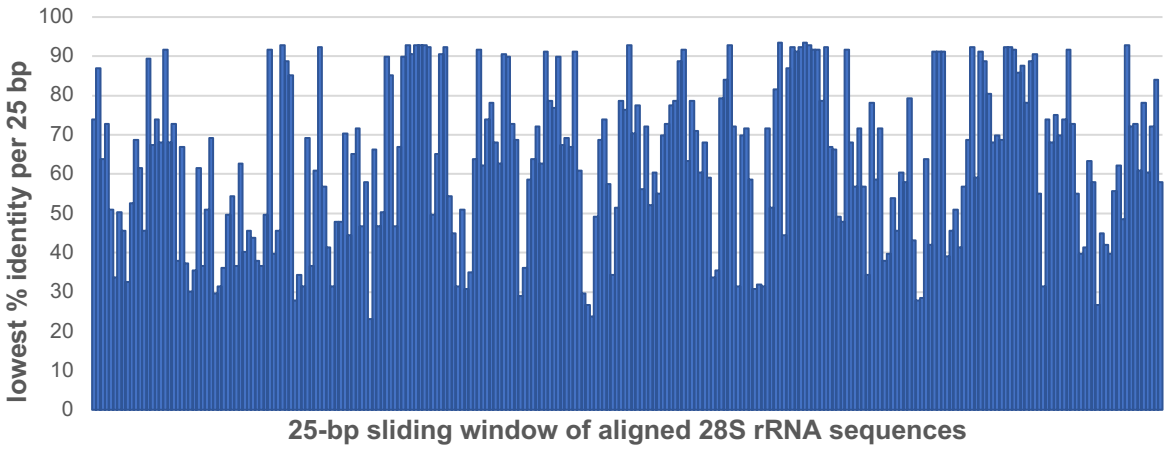

Supplementary Figure S2. Sequence conservation among 169 28S rRNA sequences obtained from this study and from GenBank combined. Multiple sequence alignment was performed on 28S rRNA sequences, 3900 bp in length. Each bar represents a 25-bp sliding window of the 28S rRNA sequence alignment where the values are the lowest percentage identity found.

626

627 **Supplementary Figure S3.** Phylogenetic tree based on 28S sequences generated from this study
628 (3900 bp) as inferred using maximum-likelihood method and constructed to scale in MEGA X (S.
629 Kumar et al., 2018) in (A) and (B) radial format. Values at each node indicate bootstrap support (%)
630 from 500 replication. Each specimen label contains information on taxonomy, origin (as indicated in 2-
631 letter country codes), and specimen ID. Label colours indicate genera: *Culex* in coral, *Anopheles* in
632 purple, *Aedes* in dark blue, *Mansonia* in dark green, *Limatus* in light green, *Coquillettidia* in light blue,
633 *Psorophora* in yellow, *Mimomyia* in teal, *Uranotaenia* in pink and *Eretmapodites* in brown. Scale bar
634 at 0.05 is shown.

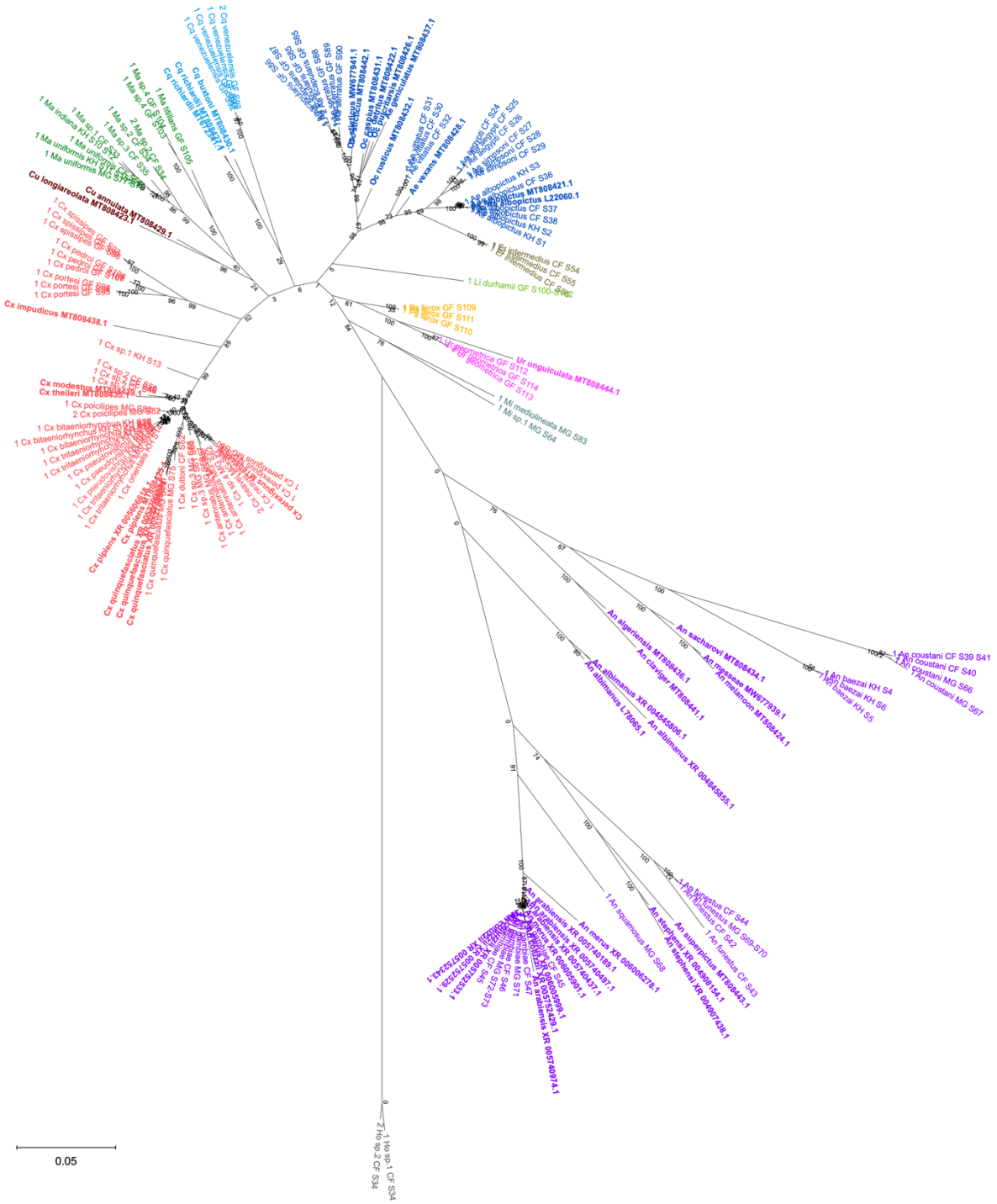

635

636 **Supplementary Figure S4.** Phylogenetic tree based on 28S sequences generated from this study
637 and from GenBank (3900 bp) as inferred using maximum-likelihood method and constructed to scale
638 in MEGA X (S. Kumar et al., 2018) in radial format to illustrate the distance of Anopheline sequences
639 relative to other Culicidae members. Values at each node indicate bootstrap support (%) from 500
640 replications. For sequences from this study, each specimen label contains information on taxonomy,
641 origin (in 2-letter country codes), and specimen ID. Labels in bold indicate GenBank sequences with

accession numbers shown. Label colours indicate genera: *Culex* in coral, *Anopheles* in purple, *Aedes* in dark blue, *Mansonia* in dark green, *Culiseta* in maroon, *Limatus* in light green, *Coquillettidia* in light blue, *Psorophora* in yellow, *Mimomyia* in teal, *Uranotaenia* in pink and *Eretmapodites* in brown. Scale bar at 0.05 is shown.

Supplementary File 1: Multiple sequence alignment of 169 28S rRNA sequences from this study and from GenBank (FASTA).

Supplementary File 2: Multiple sequence alignment of 122 28S rRNA sequences, including two sequences from *Horreolanus sp.* (FASTA).

Supplementary File 3: Multiple sequence alignment of 114 18S rRNA sequences, including two sequences from *Horreolanus sp*. (FASTA).

Supplementary File 4: Multiple sequence alignment of 106 COI sequences (FASTA).

REFERENCES

Altschul, S. F., Gish, W., Miller, W., Myers, E. W., & Lipman, D. J. (1990). Basic local alignment search tool. *Journal of Molecular Biology*, *215*(3), 403–410. https://doi.org/10.1016/S0022-2836(05)80360-2

Arctander, P. (1995). Comparison of a mitochondrial gene and a corresponding nuclear pseudogene. *Proceedings of the Royal Society B: Biological Sciences*, *262*(1363), 13–19. https://doi.org/10.1098/rspb.1995.0170

Arunachalam, N., Philip Samuel, P., Hiriyan, J., Thenmozhi, V., & Gajanana, A. (2004). Japanese encephalitis in Kerala, South India: Can Mansonia (Diptera: Culicidae) play a supplemental role in transmission? *Journal of Medical Entomology*, *41*(3), 456–461. https://doi.org/10.1603/0022-2585-41.3.456

Aspen, S., & Savage, H. M. (2003). Polymerase chain reaction assay identifies North American members of the Culex pipiens complex based on nucleotide sequence differences in the acetylcholinesterase gene Ace.2. *Journal of the American Mosquito Control Association*, *19*(4), 323–328.

Auerswald, H., Maquart, P. O., Chevalier, V., & Boyer, S. (2021). Mosquito vector competence for japanese encephalitis virus. *Viruses*, *13*(6), 1154. https://doi.org/10.3390/v13061154

Bankevich, A., Nurk, S., Antipov, D., Gurevich, A. A., Dvorkin, M., Kulikov, A. S., Lesin, V. M.,

671 Nikolenko, S. I., Pham, S., Prjibelski, A. D., Pyshkin, A. V., Sirotkin, A. V., Vyahhi, N., Tesler, G.,
672 Alekseyev, M. A., & Pevzner, P. A. (2012). SPAdes: A new genome assembly algorithm and its
673 applications to single-cell sequencing. *Journal of Computational Biology*, *19*(5), 455–477.
674 https://doi.org/10.1089/cmb.2012.0021
675 Barrio-Nuevo, K. M., Cunha, M. S., Luchs, A., Fernandes, A., Rocco, I. M., Mucci, L. F., DE Souza, R.
676 P., Medeiros-Sousa, A. R., Ceretti-Junior, W., & Marrelli, M. T. (2020). Detection of Zika and
677 dengue viruses in wildcaught mosquitoes collected during field surveillance in an environmental
678 protection area in São Paulo, Brazil. *PLoS ONE*, *15*(10), e0227239.
679 https://doi.org/10.1371/journal.pone.0227239
680 Batovska, J., Cogan, N. O. I., Lynch, S. E., & Blacket, M. J. (2017). Using next-generation sequencing
681 for DNA barcoding: Capturing allelic variation in ITS2. *G3: Genes, Genomes, Genetics*, *7*(1),
682 19–29. https://doi.org/10.1534/G3.116.036145/-/DC1
683 Beebe, N. W. (2018). DNA barcoding mosquitoes: Advice for potential prospectors. *Parasitology*,
684 *145*(5), 622–633. https://doi.org/10.1017/S0031182018000343
685 Behura, S. K. (2006). Molecular marker systems in insects: current trends and future avenues.
686 *Molecular Ecology*, *15*(11), 3087–3113. https://doi.org/10.1111/J.1365-294X.2006.03014.X
687 Belda, E., Nanfack-Minkeu, F., Eiglmeier, K., Carissimo, G., Holm, I., Diallo, M., Diallo, D., Vantaux,
688 A., Kim, S., Sharakhov, I. V., & Vernick, K. D. (2019). De novo profiling of RNA viruses in
689 Anopheles malaria vector mosquitoes from forest ecological zones in Senegal and Cambodia.
690 *BMC Genomics*, *20*(1), 664. https://doi.org/10.1186/s12864-019-6034-1
691 Bhattacharya, S., Basu, P., & Sajal Bhattacharya, C. (2016). The Southern House Mosquito, Culex
692 quinquefasciatus: profile of a smart vector. *Journal of Entomology and Zoology Studies JEZS*,
693 *4*(2), 73–81.
694 Bishop-Lilly, K. A., Turell, M. J., Willner, K. M., Butani, A., Nolan, N. M. E., Lentz, S. M., Akmal, A.,
695 Mateczun, A., Brahmbhatt, T. N., Sozhamannan, S., Whitehouse, C. A., & Read, T. D. (2010).
696 Arbovirus detection in insect vectors by Rapid, high- throughput pyrosequencing. *PLoS*
697 *Neglected Tropical Diseases*, *4*(11), e878. https://doi.org/10.1371/journal.pntd.0000878
698 Brault, A. C., Foy, B. D., Myles, K. M., Kelly, C. L. H., Higgs, S., Weaver, S. C., Olson, K. E., Miller, B.
699 R., & Powers, A. M. (2004). Infection patterns of o'nyong nyong virus in the malaria-transmitting
700 mosquito, Anopheles gambiae. *Insect Molecular Biology*, *13*(6), 625–635.

https://doi.org/10.1111/j.0962-1075.2004.00521.x

Cardoso, J. da C., de Almeida, M. A. B., dos Santos, E., da Fonseca, D. F., Sallum, M. A. M., Noll, C. A., Monteiro, H. A. d. O., Cruz, A. C. R., Carvalho, V. L., Pinto, E. V., Castro, F. C., Neto, J. P. N., Segura, M. N. O., & Vasconcelos, P. F. C. (2010). Yellow fever virus in Haemagogus leucocelaenus and Aedes serratus mosquitoes, Southern Brazil, 2008. *Emerging Infectious Diseases*, *16*(12), 1918–1924. https://doi.org/10.3201/eid1612.100608

Chandler, J. A., Liu, R. M., & Bennett, S. N. (2015). RNA Shotgun Metagenomic Sequencing of Northern California (USA) Mosquitoes Uncovers Viruses, Bacteria, and Fungi. *Frontiers in Microbiology*, *6*, 185. https://doi.org/10.3389/fmicb.2015.00185

Cornel, A. J., Mcabee, R. D., Rasgon, J., Stanich, M. A., Scott, T. W., & Coetzee, M. (2003). Differences in Extent of Genetic Introgression between Sympatric Culex pipiens and Culex quinquefasciatus (Diptera: Culicidae) in California and South Africa. *Journal of Medical Entomology*, *40*(1), 36–51. https://doi.org/10.1603/0022-2585-40.1.36

Danforth, B. N., Lin, C. P., & Fang, J. (2005). How do insect nuclear ribosomal genes compare to protein-coding genes in phylogenetic utility and nucleotide substitution patterns? *Systematic Entomology*, *30*(4), 549–562. https://doi.org/10.1111/J.1365-3113.2005.00305.X

De Oliveira, C. D., Gonçalves, D. S., Baton, L. A., Shimabukuro, P. H. F., Carvalho, F. D., & Moreira, L. A. (2015). Broader prevalence of Wolbachia in insects including potential human disease vectors. *Bulletin of Entomological Research*, *105*(3), 305–315. https://doi.org/10.1017/S0007485315000085

Diallo, D., Fall, G., Diagne, C. T., Gaye, A., Ba, Y., Dia, I., Faye, O., & Diallo, M. (2020). Concurrent amplification of Zika, chikungunya, and yellow fever virus in a sylvatic focus of arboviruses in Southeastern Senegal, 2015. *BMC Microbiology*, *20*, 181. https://doi.org/10.1186/s12866-020-01866-9

Edgar, R. C. (2004). MUSCLE: A multiple sequence alignment method with reduced time and space complexity. *BMC Bioinformatics*, *5*, 113. https://doi.org/10.1186/1471-2105-5-113

Farajollahi, A., Fonseca, D. M., Kramer, L. D., & Marm Kilpatrick, A. (2011). “Bird biting” mosquitoes and human disease: A review of the role of Culex pipiens complex mosquitoes in epidemiology. *Infection, Genetics and Evolution*, *11*(7), 1577–1585. doi: 10.1016/j.meegid.2011.08.013

Fauver, J. R., Akter, S., Morales, A. I. O., Black, W. C., Rodriguez, A. D., Stenglein, M. D., Ebel, G.

731 D., & Weger-Lucarelli, J. (2019). A reverse-transcription/RNase H based protocol for depletion of
732 mosquito ribosomal RNA facilitates viral intrahost evolution analysis, transcriptomics and
733 pathogen discovery. *Virology*, *528*, 181–197. https://doi.org/10.1016/j.virol.2018.12.020
734 Foley, D. H., Rueda, L. M., & Wilkerson, R. C. (2007). Insight into Global Mosquito Biogeography from
735 Country Species Records. *Journal of Medical Entomology*, *44*(4), 554–567.
736 https://doi.org/10.1093/JMEDENT/44.4.554
737 Folmer, O., Black, M., Hoeh, W., Lutz, R., & Vrijenhoek, R. (1994). DNA primers for amplification of
738 mitochondrial cytochrome c oxidase subunit I from diverse metazoan invertebrates. *Molecular*
739 *Marine Biology and Biotechnology*, *3*(5), 294–299.
740 Gaillet, M., Pichard, C., Restrepo, J., Lavergne, A., Perez, L., Enfissi, A., Abboud, P., Lambert, Y.,
741 Ma, L., Monot, M., Demar, M., Djossou, F., Servas, V., Nacher, M., Andrieu, A., Prudhomme, J.,
742 Michaud, C., Rousseau, C., Jeanne, I., … Rousset, D. (2021). Outbreak of oropouche virus in
743 french guiana. *Emerging Infectious Diseases*, *27*(10), 2711–2714.
744 https://doi.org/10.3201/eid2710.204760
745 Gale, K., & Crampton, J. (1989). The ribosomal genes of the mosquito, Aedes aegypti. *European*
746 *Journal of Biochemistry*, *185*(2), 311–317. https://doi.org/10.1111/j.1432-1033.1989.tb15117.x
747 Hajibabaei, M., Singer, G. A. C., & Hickey, D. A. (2006). Benchmarking DNA barcodes: An
748 assessment using available primate sequences. *Genome*, *49*(7), 851–854.
749 https://doi.org/10.1139/G06-025/SUPPL_FILE/G06-025B.PDF
750 Harbach, R. E. (2007). The Culicidae (Diptera): A review of taxonomy, classification and phylogeny.
751 *Zootaxa*, *1668*(1), 591–638. https://doi.org/10.11646/zootaxa.1668.1.28
752 Harbach, R. E., Culverwell, C. L., & Kitching, I. J. (2017). Phylogeny of the nominotypical subgenus of
753 Culex (Diptera: Culicidae): insights from analyses of anatomical data into interspecific
754 relationships and species groups in an unresolved tree. *Systematics and Biodiversity*, *15*(4),
755 296–306. https://doi.org/10.1080/14772000.2016.1252439
756 Harbach, R. E., & Kitching, I. J. (2016). The phylogeny of Anophelinae revisited: Inferences about the
757 origin and classification of Anopheles (Diptera: Culicidae). *Zoologica Scripta*, *45*(1), 34–47.
758 https://doi.org/10.1111/zsc.12137
759 Hebert, P. D. N., Cywinska, A., Ball, S. L., & DeWaard, J. R. (2003). Biological identifications through
760 DNA barcodes. *Proceedings of the Royal Society B: Biological Sciences*, *270*(1512), 313–321.

761 https://doi.org/10.1098/rspb.2002.2218

762 Hoyos-López, R., Soto, S. U., Rúa-Uribe, G., & Gallego-Gómez, J. C. (2015). Molecular identification
763 of saint louis encephalitis virus genotype IV in Colombia. *Memorias Do Instituto Oswaldo Cruz*,
764 *110*(6), 719–725. https://doi.org/10.1590/0074-02760280040

765 Hurst, G. D. D., & Jiggins, F. M. (2005). Problems with mitochondrial DNA as a marker in population,
766 phylogeographic and phylogenetic studies: The effects of inherited symbionts. *Proceedings of*
767 *the Royal Society B: Biological Sciences*, *272*, 1525–1534.
768 https://doi.org/10.1098/rspb.2005.3056

769 Kim, H., Cha, G. W., Jeong, Y. E., Lee, W. G., Chang, K. S., Roh, J. Y., Yang, S. C., Park, M. Y.,
770 Park, C., & Shin, E. H. (2015). Detection of Japanese encephalitis virus genotype V in Culex
771 orientalis and Culex pipiens (Diptera: Culicidae) in Korea. *PLoS ONE*, *10*(2), e0116547.
772 https://doi.org/10.1371/journal.pone.0116547

773 Kraemer, M. U. G., Reiner, R. C., Brady, O. J., Messina, J. P., Gilbert, M., Pigott, D. M., Yi, D.,
774 Johnson, K., Earl, L., Marczak, L. B., Shirude, S., Davis Weaver, N., Bisanzio, D., Perkins, T. A.,
775 Lai, S., Lu, X., Jones, P., Coelho, G. E., Carvalho, R. G., … Golding, N. (2019). Past and future
776 spread of the arbovirus vectors Aedes aegypti and Aedes albopictus. *Nature Microbiology*, *4*(5),
777 854–863. https://doi.org/10.1038/s41564-019-0376-y

778 Kukutla, P., Steritz, M., & Xu, J. (2013). Depletion of ribosomal RNA for mosquito gut metagenomic
779 RNA-seq. *Journal of Visualized Experiments*, *74*, 50093. https://doi.org/10.3791/50093

780 Kumar, N., Creasy, T., Sun, Y., Flowers, M., Tallon, L. J., & Dunning Hotopp, J. C. (2012). Efficient
781 subtraction of insect rRNA prior to transcriptome analysis of Wolbachia-Drosophila lateral gene
782 transfer. *BMC Research Notes*, *5*, 230. https://doi.org/10.1186/1756-0500-5-230

783 Kumar, S., Stecher, G., Li, M., Knyaz, C., & Tamura, K. (2018). MEGA X: Molecular evolutionary
784 genetics analysis across computing platforms. *Molecular Biology and Evolution*, *35*(6), 1547–
785 1549. https://doi.org/10.1093/molbev/msy096

786 Logue, K., Chan, E. R., Phipps, T., Small, S. T., Reimer, L., Henry-Halldin, C., Sattabongkot, J., Siba,
787 P. M., Zimmerman, P. A., & Serre, D. (2013). Mitochondrial genome sequences reveal deep
788 divergences among Anopheles punctulatus sibling species in Papua New Guinea. *Malaria*
789 *Journal*, *12*(1), 1–11. https://doi.org/10.1186/1475-2875-12-64/FIGURES/3

790 Lorenz, C., Alves, J. M. P., Foster, P. G., Suesdek, L., & Sallum, M. A. M. (2021). Phylogeny and

temporal diversification of mosquitoes (Diptera: Culicidae) with an emphasis on the Neotropical fauna. *Systematic Entomology*, *46*(4), 798–811. https://doi.org/10.1111/SYEN.12489

Lutomiah, J., Bast, J., Clark, J., Richardson, J., Yalwala, S., Oullo, D., Mutisya, J., Mulwa, F., Musila, L., Khamadi, S., Schnabel, D., Wurapa, E., & Sang, R. (2013). Abundance, diversity, and distribution of mosquito vectors in selected ecological regions of Kenya: Public health implications. *Journal of Vector Ecology*, *38*(1), 134–142. https://doi.org/10.1111/j.1948-7134.2013.12019.x

Madeira, F., Park, Y. M., Lee, J., Buso, N., Gur, T., Madhusoodanan, N., Basutkar, P., Tivey, A. R. N., Potter, S. C., Finn, R. D., & Lopez, R. (2019). The EMBL-EBI search and sequence analysis tools APIs in 2019. *Nucleic Acids Research*, *47*(W1), W636–W641. https://doi.org/10.1093/nar/gkz268

Maquart, P. O., & Boyer, S. (2022). Culex vishnui. *Trends in Parasitology*, *Vector of the Month*, 491–492. https://doi.org/10.1016/J.PT.2022.01.003

Maquart, P. O., Sokha, C., & Boyer, S. (2021). Mosquito diversity (Diptera: Culicidae) and medical importance, in a bird sanctuary inside the flooded forest of Prek Toal, Cambodia. *Journal of Asia-Pacific Entomology*, *24*(4), 1221–1227. https://doi.org/10.1016/j.aspen.2021.08.001

Mitchell, C. J., Forattini, O. P., & Miller, B. R. (1986). Vector competence experiments with Rocio virus and three mosquito species from the epidemic zone in Brazil. *Revista de Saúde Pública*, *20*(3), 171–177. https://doi.org/10.1590/s0034-89101986000300001

Morlan, J. D., Qu, K., & Sinicropi, D. V. (2012). Selective depletion of rRNA enables whole transcriptome profiling of archival fixed tissue. *PLoS ONE*, *7*(8), e42882. https://doi.org/10.1371/journal.pone.0042882

Mukwaya, L. G., Kayondo, J. K., Crabtree, M. B., Savage, H. M., Biggerstaff, B. J., & Miller, B. R. (2000). Genetic differentiation in the yellow fever virus vector, Aedes simpsoni complex, in Africa: Sequence variation in the ribosomal DNA internal transcribed spacers of anthropophilic and non-anthropophilic populations. *Insect Molecular Biology*, *9*(1), 85–91. doi: 10.1046/j.1365-2583.2000.00161.x

Mwangangi, J. M., Muturi, E. J., Muriu, S. M., Nzovu, J., Midega, J. T., & Mbogo, C. (2013). The role of Anopheles arabiensis and Anopheles coustani in indoor and outdoor malaria transmission in Taveta District, Kenya. *Parasites and Vectors*, *6*, 114. https://doi.org/10.1186/1756-3305-6-114

821 Navarro, J. C., & Weaver, S. C. (2004). Molecular phylogeny of the Vomerifer and Pedroi Groups in
822 the spissipes section of the subgenus Culex (Melanoconion). *Journal of Medical Entomology*,
823 *41*(4), 575–581. https://doi.org/10.1603/0022-2585-41.4.575
824 Nchoutpouen, E., Talipouo, A., Djiappi-Tchamen, B., Djamouko-Djonkam, L., Kopya, E., Ngadjeu, C.
825 S., Doumbe-Belisse, P., Awono-Ambene, P., Kekeunou, S., Wondji, C. S., & Antonio-Nkondjio,
826 C. (2019). Culex species diversity, susceptibility to insecticides and role as potential vector of
827 Lymphatic filariasis in the city of Yaoundé, Cameroon. *PLoS Neglected Tropical Diseases*,
828 *13*(4), e0007229. https://doi.org/10.1371/journal.pntd.0007229
829 Ndiaye, E. H., Fall, G., Gaye, A., Bob, N. S., Talla, C., Diagne, C. T., Diallo, D., Ba, Y., Dia, I., Kohl,
830 A., Sall, A. A., & Diallo, M. (2016). Vector competence of Aedes vexans (Meigen), Culex
831 poicilipes (Theobald) and Cx. quinquefasciatus Say from Senegal for West and East African
832 lineages of Rift Valley fever virus. *Parasites and Vectors*, *9*, 94. https://doi.org/10.1186/s13071-
833 016-1383-y
834 Nepomichene, T. N. J. J., Raharimalala, F. N., Andriamandimby, S. F., Ravalohery, J. P., Failloux, A.
835 B., Heraud, J. M., & Boyer, S. (2018). Vector competence of Culex antennatus and Anopheles
836 coustani mosquitoes for Rift Valley fever virus in Madagascar. *Medical and Veterinary*
837 *Entomology*, *32*(2), 259–262. https://doi.org/10.1111/mve.12291
838 Nikolay, B., Diallo, M., Boye, C. S. B., & Sall, A. A. (2011). Usutu virus in Africa. *Vector-Borne and*
839 *Zoonotic Diseases*, *11*(11), 1417–1423. https://doi.org/10.1089/vbz.2011.0631
840 Phelps, W. A., Carlson, A. E., & Lee, M. T. (2021). Optimized design of antisense oligomers for
841 targeted rRNA depletion. *Nucleic Acids Research*, *49*(1), e5.
842 https://doi.org/10.1093/nar/gkaa1072
843 Quast, C., Pruesse, E., Yilmaz, P., Gerken, J., Schweer, T., Yarza, P., Peplies, J., & Glöckner, F. O.
844 (2013). The SILVA ribosomal RNA gene database project: Improved data processing and web-
845 based tools. *Nucleic Acids Research*, *41*(Database issue), D590–D596.
846 https://doi.org/10.1093/nar/gks1219
847 Ratnasingham, S., & Hebert, P. D. N. (2007). BOLD: The Barcode of Life Data System: Barcoding.
848 *Molecular Ecology Notes*, *7*(3), 355–364. https://doi.org/10.1111/j.1471-8286.2007.01678.x
849 Ratovonjato, J., Olive, M. M., Tantely, L. M., Andrianaivolambo, L., Tata, E., Razainirina, J.,
850 Jeanmaire, E., Reynes, J. M., & Elissa, N. (2011). Detection, isolation, and genetic

characterization of Rift Valley fever virus from anopheles (Anopheles) coustani, anopheles (Anopheles) squamosus, and culex (Culex) antennatus of the haute matsiatra region, Madagascar. *Vector-Borne and Zoonotic Diseases*, *11*(6), 753–759. https://doi.org/10.1089/vbz.2010.0031

Rausch, T., Fritz, M. H. Y., Untergasser, A., & Benes, V. (2020). Tracy: Basecalling, alignment, assembly and deconvolution of sanger chromatogram trace files. *BMC Genomics*, *21*(1), 230. https://doi.org/10.1186/s12864-020-6635-8

Rausch, T., Hsi-Yang Fritz, M., Korbel, J. O., & Benes, V. (2019). Alfred: Interactive multi-sample BAM alignment statistics, feature counting and feature annotation for long- and short-read sequencing. *Bioinformatics*, *35*(14), 2489–2491. https://doi.org/10.1093/bioinformatics/bty1007

Reidenbach, K. R., Cook, S., Bertone, M. A., Harbach, R. E., Wiegmann, B. M., & Besansky, N. J. (2009). Phylogenetic analysis and temporal diversification of mosquitoes (Diptera: Culicidae) based on nuclear genes and morphology. *BMC Evolutionary Biology*, *9*(1), 1–14. https://doi.org/10.1186/1471-2148-9-298/FIGURES/4

Ruzzante, L., Reijnders, M. J. M. F., & Waterhouse, R. M. (2019). Of Genes and Genomes: Mosquito Evolution and Diversity. *Trends in Parasitology*, *35*(1), 32–51. https://doi.org/10.1016/J.PT.2018.10.003/ATTACHMENT/B9BE6BC5-D73A-4FEF-A654-CC1374C59925/MMC1.MP4

Sallum, M. A. M., & Forattini, O. P. (1996). Revision of the Spissipes Section of Culex (Melanoconion) (diptera: Culicidae). *Journal of the American Mosquito Control Association*, *12*(3), 517–600.

Sirivanakarn, S. (1982). A review of the Systematics and a Proposed Scheme of Internal Classification of the New World Subgenus Melanoconion of Culex (Diptera, Culicidae). *Mosquito Systematics*, *14*(4), 265–333.

Stevenson, J. C., Simubali, L., Mbambara, S., Musonda, M., Mweetwa, S., Mudenda, T., Pringle, J. C., Jones, C. M., & Norris, D. E. (2016). Detection of plasmodium falciparum infection in anopheles squamosus (diptera: Culicidae) in an area targeted for malaria elimination, Southern Zambia. *Journal of Medical Entomology*, *53*(6), 1482–1487. https://doi.org/10.1093/jme/tjw091

Sun, L., Li, T. J., Fu, W. B., Yan, Z. T., Si, F. L., Zhang, Y. J., Mao, Q. M., Demari-Silva, B., & Chen, B. (2019). The complete mt genomes of Lutzia halifaxia, Lt. fuscanus and Culex pallidothorax (Diptera: Culicidae) and comparative analysis of 16 Culex and Lutzia mt genome sequences.

Parasites and Vectors, *12*, 368. https://doi.org/10.1186/s13071-019-3625-2

Takhampunya, R., Kim, H. C., Tippayachai, B., Kengluecha, A., Klein, T. A., Lee, W. J., Grieco, J., & Evans, B. P. (2011). Emergence of Japanese encephalitis virus genotype v in the Republic of Korea. *Virology Journal*, *8*, 449. https://doi.org/10.1186/1743-422X-8-449

Talaga, S., Duchemin, J. B., Girod, R., & Dusfour, I. (2021). The Culex Mosquitoes (Diptera: Culicidae) of French Guiana: A Comprehensive Review With the Description of Three New Species. *Journal of Medical Entomology*, *58*(1), 182–221. https://doi.org/10.1093/JME/TJAA205

Thongsripong, P., Chandler, J. A., Kittayapong, P., Wilcox, B. A., Kapan, D. D., & Bennett, S. N. (2021). Metagenomic shotgun sequencing reveals host species as an important driver of virome composition in mosquitoes. *Scientific Reports*, *11*(1), 8448. https://doi.org/10.1038/s41598-021-87122-0

Torres-Gutierrez, C., Bergo, E. S., Emerson, K. J., de Oliveira, T. M. P., Greni, S., & Sallum, M. A. M. (2016). Mitochondrial COI gene as a tool in the taxonomy of mosquitoes Culex subgenus Melanoconion. *Acta Tropica*, *164*, 137–149. https://doi.org/10.1016/j.actatropica.2016.09.007

Torres-Gutierrez, C., De Oliveira, T. M. P., Emerson, K. J., Bergo, E. S., & Sallum, M. A. M. (2018). Molecular phylogeny of Culex subgenus Melanoconion (Diptera: Culicidae) based on nuclear and mitochondrial protein-coding genes. *Royal Society Open Science*, *5*, 171900. https://doi.org/10.1098/rsos.171900

Turell, M. J., O'guinn, M. L., Dohm, D., Zyzak, M., Watts, D., Fernandez, R., Calampa, C., Klein, T. A., & Jones, J. W. (2008). Susceptibility of Peruvian Mosquitoes to Eastern Equine Encephalitis Virus. *Journal of Medical Entomology*, *45*(4), 720–725. https://doi.org/10.1093/JMEDENT/45.4.720

Turell, Michael J. (1999). Vector competence of three Venezuelan mosquitoes (Diptera: Culicidae) for an epizootic IC strain of Venezuelan equine encephalitis virus. *Journal of Medical Entomology*, *36*(4), 407–409. https://doi.org/10.1093/jmedent/36.4.407

Ughasi, J., Bekard, H. E., Coulibaly, M., Adabie-Gomez, D., Gyapong, J., Appawu, M., Wilson, M. D., & Boakye, D. A. (2012). Mansonia africana and Mansonia uniformis are Vectors in the transmission of Wuchereria bancrofti lymphatic filariasis in Ghana. *Parasites and Vectors*, *5*(1), 1–5. https://doi.org/10.1186/1756-3305-5-89

Valentine, M. J., Murdock, C. C., & Kelly, P. J. (2019). Sylvatic cycles of arboviruses in non-human

911 primates. *Parasites and Vectors*, *12*(1), 1–18. https://doi.org/10.1186/S13071-019-3732-
912 0/TABLES/4
913 Vasconcelos, P. F. C., Costa, Z. G., Travassos da Rosa, E. S., Luna, E., Rodrigues, S. G., Barros, V.
914 L. R. S., Dias, J. P., Monteiro, H. A. O., Oliva, O. F. P., Vasconcelos, H. B., Oliveira, R. C.,
915 Sousa, M. R. S., Barbosa Da Silva, J., Cruz, A. C. R., Martins, E. C., & Travassos Da Rosa, J.
916 F. S. (2001). Epidemic of jungle yellow fever in Brazil, 2000: Implications of climatic alterations in
917 disease spread. *Journal of Medical Virology*, *65*(3), 598–604.
918 https://doi.org/10.1002/jmv.2078.abs
919 Vázquez González, A., Ruiz, S., Herrero, L., Moreno, J., Molero, F., Magallanes, A., Sánchez-Seco,
920 M. P., Figuerola, J., & Tenorio, A. (2011). West Nile and Usutu viruses in mosquitoes in Spain,
921 2008-2009. *American Journal of Tropical Medicine and Hygiene*, *85*(1), 178–181.
922 https://doi.org/10.4269/ajtmh.2011.11-0042
923 Vezenegho, S. B., Issaly, J., Carinci, R., Gaborit, P., Girod, R., Dusfour, I., & Briolant, S. (2022).
924 Discrimination of 15 Amazonian Anopheline Mosquito Species by Polymerase Chain Reaction—
925 Restriction Fragment Length Polymorphism. *Journal of Medical Entomology*, *59*(3), 1060–1064.
926 https://doi.org/10.1093/JME/TJAC008
927 Weaver, S. C., Ferro, C., Barrera, R., Boshell, J., & Navarro, J. C. (2004). Venezuelan Equine
928 Encephalitis. *Annual Review of Entomology*, *49*, 141–174.
929 https://doi.org/10.1146/annurev.ento.49.061802.123422
930 Webster, J. P., Gower, C. M., Knowles, S. C. L., Molyneux, D. H., & Fenton, A. (2016). One health -
931 an ecological and evolutionary framework for tackling Neglected Zoonotic Diseases.
932 *Evolutionary Applications*, *9*(2), 313–333. https://doi.org/10.1111/eva.12341
933 Weedall, G. D., Irving, H., Hughes, M. A., & Wondji, C. S. (2015). Molecular tools for studying the
934 major malaria vector Anopheles funestus: Improving the utility of the genome using a
935 comparative poly(A) and Ribo-Zero RNAseq analysis. *BMC Genomics*, *16*(1), 931.
936 https://doi.org/10.1186/s12864-015-2114-z
937 WHO. (2017). Global vector control response 2017–2030. In *World Health Organization*.
938 Zakrzewski, M., Rašić, G., Darbro, J., Krause, L., Poo, Y. S., Filipović, I., Parry, R., Asgari, S., Devine,
939 G., & Suhrbier, A. (2018). Mapping the virome in wild-caught Aedes aegypti from Cairns and
940 Bangkok. *Scientific Reports*, *8*(1), 4690. https://doi.org/10.1038/s41598-018-22945-y

941 Zittra, C., Flechl, E., Kothmayer, M., Vitecek, S., Rossiter, H., Zechmeister, T., & Fuehrer, H. P.
942 (2016). Ecological characterization and molecular differentiation of Culex pipiens complex taxa
943 and Culex torrentium in eastern Austria. *Parasites and Vectors*, *9*, 197.
944 https://doi.org/10.1186/s13071-016-1495-4
945

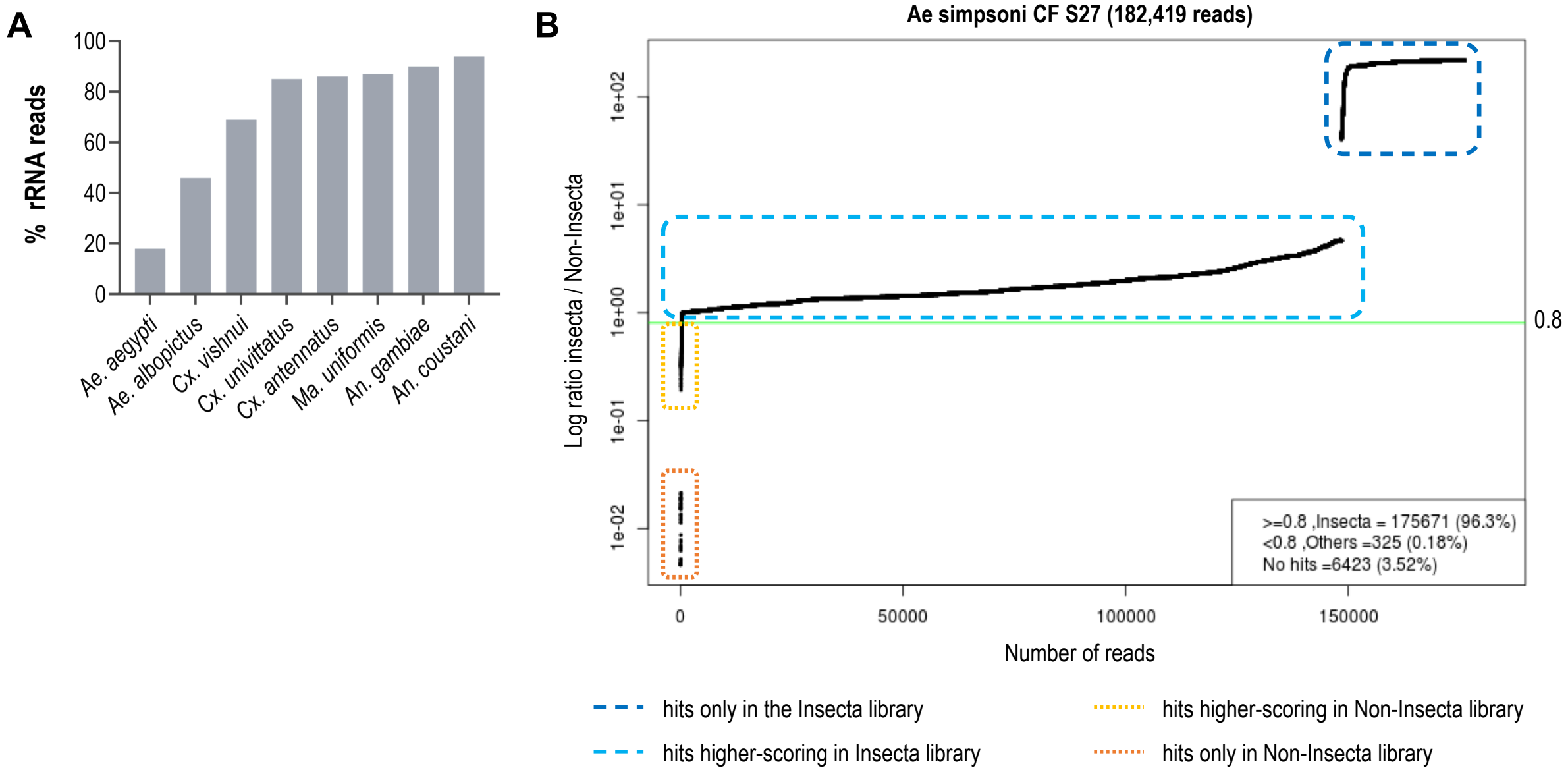
A
% rRNA reads
100
80
60
40
20
0
Ae. aegypti
Ae. albopictus
Cx. vishnui
Cx. univittatus
Cx. antennatus
Ma. uniformis
An. gambiae
An. coustani
B
Ae simpsoni CF S27 (182,419 reads)
Log ratio insecta / Non-Insecta
1e+02
1e+01
1e+00
1e-01
1e-02
0.8
>=0.8 ,Insecta = 175671 (96.3%)
<0.8 ,Others =325 (0.18%)
No hits =6423 (3.52%)
0
50000
100000
150000
Number of reads
hits only in the Insecta library
hits higher-scoring in Insecta library
hits higher-scoring in Non-Insecta library
hits only in Non-Insecta library

Cx sp.4 MG S62
Cx poicilipes MG S82
Cx pseudovishnui KH S7–S9; Cx tritaeniorhynchus KH S21–S23
Cx tritaeniorhynchus MG S115
Cx orientalis KH S14
Cx bitaeniorhynchus KH S18–S20
Cx quinquefasciatus MG S75
Cx sp.2 CF S48, S50
Cx sp.2 CF S49
Cx neavei MG S84
Cx sp.3 MG S61, S65
Cx sp.3 MG S63
Cx perexiguus MG S76
Cx duttoni CF S52
Cx perexiguus MG S60
Cx antennatus MG S57, S59
Cx antennatus MG S58
Ma sp.3 CF S35
Cx quinquefasciatus MG S74
Cx sp.1 KH S13
Cx portesi GF S94
Cx portesi GF S95, S96
Cx pedroi GF S106, S108
Cx pedroi GF S107
Cx spissipes GF S97–S99

subgenus *Melanoconion*

Ps ferox GF S109, S110
Ps ferox GF S111
Ae scapularis GF S85, S86
Ae sp.4 KH S19 GF S87
Ae serratus GF S88, S90

subgenus *Ochlerotatus*

Ae aegypti CF S25, S26
Ae aegypti CF S24
Ae albopictus KH S1, S3
Ae albopictus CF S36–S38; Ae albopictus KH S2
Ae simpsoni CF S27, S28
Ae simpsoni CF S29
Ae vittatus CF S30
Ae vittatus CF S32
Ae vittatus CF S31

subgenus *Stegomyia*

Er intermedius CF S54–S56
Ma uniformis CF S51 MG S77, S78
Ma uniformis KH S15
Ma uniformis KH S11, S16, S17
Ma indiana KH S10, S12
Ma uniformis MG S79
Ma sp.1 CF S33
Ma sp.2 CF S34
Ma sp.4 GF S103
Ma sp.4 GF S104
Ma titillans GF S105

subgenus *Mansonoides*

Ur geometrica GF S112–S114
Mi sp.1 MG S64
Cq venezuelensis GF S91, S92
Cq venezuelensis GF S93
Mi mediolineata MG S83
Li durhamii GF S100
Li durhamii GF S101, S102
An coustani CF S39, S40; An coustani MG S67
An coustani CF S41; An coustani MG S66
An baezai KH S4–S6

subgenus *Anopheles*

An funestus CF S43
An funestus MG S69
An funestus CF S42
An funestus CF S44; An funestus MG S70
An gambiae CF S45, S46; An gambiae MG S71–S73
An gambiae CF S47
An squamosus MG S68

subgenus *Cellia*

Ho sp.1 CF S34
Ho sp.2 CF S35

0.05